Environmental Science

AIMS Environmental Science, 13(5): 936–975.
DOI: 10.3934/environsci.2026037
Received: 15 August 2026
Revised: 15 September 2026
Accepted: 22 September 2026
Published: 10 October 2026

https://www.aimspress.com/journal/environmental

Review

Metal-based functional interfaces in membrane bioreactors for antibiotic-containing wastewater: Performance benefits and antibiotic resistance risks

Zihao Liu[1,2], Mingchao Zhu[1,2,*] and Shuping Li[1,2]

[1] Key Laboratory of Water Safety and Aquatic Ecosystem Health of the Xizang Autonomous Region, Xizang Minzu University, Xianyang 712082, China
[2] Key Laboratory of Water Pollution Control and Ecological Restoration of Xizang, National Ethnic Affairs Commission, Xizang Minzu University, Xianyang 712082, China

* **Correspondence:** Email: mczhu@xzmu.edu.cn.

Abstract: The coexistence of antibiotics, heavy metals, and antibiotic resistance genes (ARGs) in antibiotic-containing wastewater poses a coupled challenge for membrane bioreactors (MBRs): Treatment performance must improve without shifting environmental risk elsewhere in the system. In this review, we examined how metal-based functional interfaces influence antibiotic removal, membrane fouling, and antibiotic-resistance risks in MBRs. Metal ions, iron-based particles, functionalized membranes, and electrochemical or bioelectrochemical interfaces can enhance pollutant removal and operational stability through coagulation and adsorption, redox reactions, electron transfer, and regulation of membrane-surface interactions. However, lower concentrations of parent antibiotics or lower ARG abundances in the effluent do not necessarily reflect genuine degradation or reduced environmental risk. Pollutants and resistance determinants may accumulate in sludge, cake layers, and membrane biofilms, while metal-induced selection can favor co-resistance and cross-resistance and trigger co-regulatory responses. We proposed an integrated assessment framework that considers pollutant transformation, membrane operation, metal release, the spatial distribution of resistance determinants, and their potential for dissemination. This framework provides a basis for evaluating the long-term safety of metal-based functional interfaces in MBRs.

Keywords: membrane bioreactor; antibiotic-containing wastewater; metal-based functional interfaces; membrane fouling; antibiotic resistance genes; co-selection

Abbreviations

AnEMBR: anaerobic electrochemical membrane bioreactor; AnMBR: anaerobic membrane bioreactor; ARB: antibiotic-resistant bacteria; ARG: antibiotic resistance gene; BDD: boron-doped diamond; CAP: chloramphenicol; CIP: ciprofloxacin; CNO: carbon nano-onion; COD: chemical oxygen demand; CTC: chlortetracycline; eDNA: extracellular DNA; EET: extracellular electron transfer; eMBR/EMBR: electrochemical membrane bioreactor; EPS: extracellular polymeric substances; FQ: fluoroquinolone; HGT: horizontal gene transfer; HRMS: high-resolution mass spectrometry; ICP-MS: inductively coupled plasma mass spectrometry; LB-EPS: loosely bound extracellular polymeric substances; LC-MS/MS: liquid chromatography-tandem mass spectrometry; MABR: membrane-aerated biofilm reactor; MBBR: moving-bed biofilm reactor; MBC: magnetic biochar; MBR: membrane bioreactor; MEMBR: moving-bed electrochemical membrane bioreactor; MFC: microbial fuel cell; MFC-MBR: microbial fuel cell-membrane bioreactor; MGE: mobile genetic element; MLSS: mixed liquor suspended solids; MLSB: macrolide-lincosamide-streptogramin B; MRG: metal resistance gene; NOR: norfloxacin; NTU: nephelometric turbidity unit; nZVI: nano-zero-valent iron; OPEX: operating expenditure; PPCP: pharmaceutical and personal care product; PVDF: polyvinylidene fluoride; qPCR: quantitative polymerase chain reaction; RND: resistance-nodulation-division; ROS: reactive oxygen species; SBR: sequencing batch reactor; SDZ: sulfadiazine; SMP: soluble microbial products; SMX: sulfamethoxazole; SRT: solids retention time; TA-Cu: tannic acid-copper; TB-EPS: tightly bound extracellular polymeric substances; TC: tetracycline; TMP: transmembrane pressure; TP: transformation product; VSS: volatile suspended solids; XPS: X-ray photoelectron spectroscopy; XRD: X-ray diffraction; ZVI: zero-valent iron.

1. Introduction

Antibiotic-containing wastewater is a resistance problem as well as a contaminant-removal problem. Residual pharmaceuticals can coexist with antibiotic-resistant bacteria (ARB), antibiotic resistance genes (ARGs), and mobile genetic elements (MGEs), while heavy metals add a second selective pressure that can maintain resistance [1,2]. Extensive antibiotic use in healthcare, livestock farming, aquaculture, and pharmaceutical production releases parent compounds into aquatic environments and generates diverse transformation products (TPs) during transport and treatment [3–5]. Livestock and poultry operations are major sources of antibiotic residues and ARGs entering the environment [6–8]. Municipal wastewater treatment plants act as important nodes for their transport, transformation, and dissemination [9]. In complex wastewaters, coexisting metals such as Cu^{2+} and Zn^{2+} can intensify antibiotic selection and metal-mediated co-selection [10]. Studies of membrane-based treatment have documented pharmaceutical fate and partitioning [11], and carbamazepine illustrates the persistence of some pharmaceuticals during conventional wastewater treatment [12]. MBRs provide high biomass retention, efficient solid–liquid separation, and stable effluent quality [13,14]. Those same retention processes also shape fouling and resistance fate: EPS, SMP, and foulant layers govern membrane fouling [15], membrane foulants can retain ARGs and alter their release [16], Fe^{3+} conditioning can change pollutant removal and fouling simultaneously [17], and biofilm formation can facilitate horizontal gene transfer [18]. Effective treatment must address pollutant transformation, membrane stability, and resistance dissemination as linked outcomes.

Metal ions, metal-based particles, metal-functionalized membranes, and metal-coupled electrochemical or bioelectrochemical interfaces have been explored as ways to improve MBR performance. Their effects span several parts of the reactor. EPS and SMP control sludge-floc and

cake-layer properties [19,20]; metal–polyphenol coordination coatings can increase membrane hydrophilicity and reduce particle adhesion [21]; and biochar can improve biological performance and ease fouling in AnMBRs treating pharmaceutical wastewater [22]. Zero-valent iron can promote antibiotic transformation through iron cycling, reductive reactions, and microbial regulation [23], while magnetic biochar can combine adsorption, electron transfer, and microbial co-metabolism [24,25]. The literature leaves three practical questions unresolved. Parent-antibiotic removal and transmembrane pressure (TMP) are often used as headline indicators, even when adsorption and retention have not been separated from genuine transformation and TP toxicity, metal release, or long-term stability has not been resolved. ARG, metal resistance gene (MRG), and MGE studies commonly track a limited target set in bulk liquid or effluent, leaving their redistribution within sludge, cake layers, and membrane biofilms poorly characterized. Evidence is also difficult to compare across interface types, locations of action, and operating conditions, especially when short-term material tests or non-MBR systems are used to explain continuously operated MBRs. The central issue is whether metal interfaces can improve antibiotic removal and fouling control while keeping resistance-dissemination risks within an acceptable range.

In this review, we focus on the coupled effects of metal-based functional interfaces on antibiotic transport and transformation, membrane-fouling control, and ARG/MGE responses in MBRs. Here, "metal-based functional interfaces" refers to metal-mediated reaction zones in which metal species directly influence antibiotic partitioning or transformation, EPS/floc/cake-layer structure, membrane-surface interactions, or microbial and electrochemical processes. The definition follows interfacial function; material form alone does not determine inclusion. Dissolved metal ions are included when they participate in complexation, bridging, precipitation, or association with EPS, sludge flocs, or cake layers; their mere presence in the bulk liquid is not enough. Because these interfaces differ in mobility, spatial organization, persistence, and dominant mechanism, they are treated as distinct configurations.

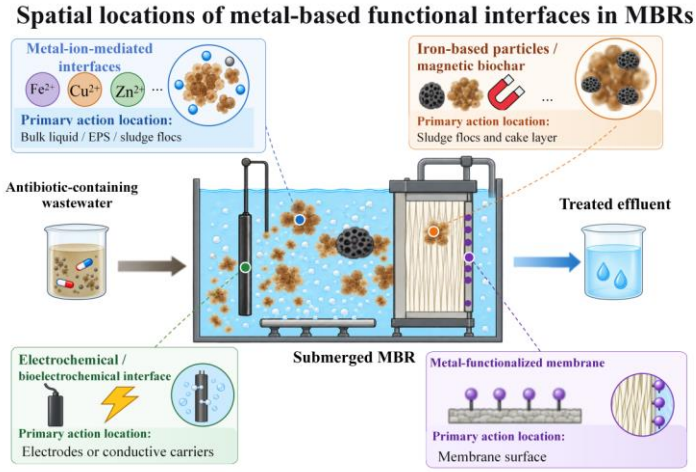


Figure 1. Schematic illustration of metal-based functional interfaces in MBRs. Depending on interface type and operating conditions, adsorption, flocculation, redox reactions, electron transfer, and membrane-surface interactions can improve antibiotic removal and fouling control while also altering antibiotic-resistance risk.

Figure 1 maps their locations of action, Table 1 summarizes their classification and functional roles, and Table 2 ranks the directness of the supporting evidence. The argument developed throughout

the review is straightforward: Metal interfaces can improve antibiotic removal and membrane performance, yet lower resistance indicators in bulk liquid or effluent do not by themselves establish lower system-level risk. Resistance determinants can persist or become enriched in retained biomass and membrane-fouling layers [16,26]. We connect pollutant transformation, fouling evolution, and resistance responses within a single benefit–risk framework for long-term operation.

Table 1. Classification of metal-based functional interfaces considered in this review.

Interface category	Representative materials/systems	Inclusion status	Primary location of action	Principal functional roles
Metal-ion-mediated interfaces	Fe^{3+}, Ca^{2+}, Cu^{2+}, Zn^{2+}	Core	Bulk liquid, EPS, sludge flocs, and cake layers	Flocculation bridging, complexation, co-precipitation, EPS regulation, and metal-associated selection pressure
Iron-based particle interfaces	$Fe(OH)_3$, nZVI, Fe_3O_4, iron oxide particles, Fe_3O_4-biochar, magnetic biochar	Core	Sludge flocs, EPS matrix, cake layers, and biofilms	Adsorption, Fe^{2+}/Fe^{3+} cycling, redox transformation, microbial co-metabolism, and fouling control
Metal-functionalized membrane interfaces	TA-Cu/PVDF, Ag@SiO_2, TA-Fe coatings, MOF-based metal-node membranes	Core*	Membrane surface, membrane biofilms, and inner cake layers	Surface-hydrophilicity regulation, interfacial adhesion control, localized metal release, antibiofouling, and local selection effects
Fe^0 self-corrosion/microelectrolysis interfaces	Fe^0-MABR, ZVI-AnMBR, iron-based microelectrolysis-coupled membrane bioreactors	Core/boundary	Fe^0 surface, iron-oxide layer, biofilms, and fouling layers	Fe^0 self-corrosion, iron cycling, microelectrolysis, electron transfer, antibiotic transformation, and ARG responses
Metal-coupled electrochemical interfaces	eMBRs/MEMBRs with metal electrodes, metal catalytic sites, or iron-based particles	Conditional/ core-related	Electrode surfaces, electrode biofilms, and fouling layers	Applied electric fields, anodic/cathodic redox reactions, electron transfer, reactive-species formation, and interfacial antibiotic transformation
Bioelectrochemical/conductive boundary interfaces	MFC-MBRs; carbon-felt-anode/stainless-steel-cathode systems	Boundary	Anodic biofilms, cathode surfaces, and fouling layers	Bioelectrochemical transformation, functional-community regulation, fouling mitigation, and spatial redistribution of ARGs

*Note: For metal-functionalized membranes, continuous-MBR studies provide the direct operational evidence; short-term membrane-material studies are used only for mechanism. "Boundary" or "conditional" inclusion identifies systems in which the metal component is coupled with broader electrochemical or bioelectrochemical functions.

Table 2. Evidence-strength hierarchy for evaluating metal-based functional interfaces in MBRs.

Evidence category	Relative evidence strength	Typical evidence source	Relevance to MBR operation	Role in this review	Evidence boundary
Direct continuous-MBR evidence	High	Continuously operated MBRs/AnMBRs/eMBRs using metal ions, metal particles, metal-functionalized membranes, or metal-coupled electrochemical interfaces	Directly reflects membrane operation, sludge retention, fouling evolution, and effluent performance under MBR conditions	Primary basis for conclusions on antibiotic removal, membrane-fouling control, operational stability, and ARG/MGE responses	Coverage is concentrated on specific antibiotics, selected ARGs, short-to-medium operating periods, and laboratory-scale systems
Membrane-coupled reactor evidence	Moderate to high	Fe^0-MABR, microelectrolysis-enhanced membrane-coupled reactors, and related membrane-associated systems	Retains important membrane/biofilm/interfacial features but may differ from conventional submerged MBR configuration	Supports interpretation of iron cycling, electron transfer, antibiotic transformation, and ARG responses	Reactor configuration and transport conditions differ from conventional submerged MBRs
Related biofilm or activated-sludge evidence	Supporting	SBRs, activated-sludge reactors, river biofilms, three-dimensional biofilm-electrode reactors, and metal-stressed microbial systems	Captures microbial stress, co-selection, MGE activation, and biofilm-related responses, but lacks the complete MBR retention/fouling environment	Used to support mechanisms of metal co-selection, cross-resistance, co-regulation, host enrichment, and ARG/MGE dissemination	Provides indirect support for responses in MBR sludge, cake layers, and membrane biofilms
Non-MBR mechanistic evidence	Mechanistic/ supporting	Independent adsorption, catalytic, Fenton/photo-Fenton, advanced oxidation, and electrochemical degradation experiments	Provides detailed transformation pathways and reaction mechanisms but does not reproduce MBR operating conditions	Used to explain antibiotic transformation pathways, TP formation, redox mechanisms, and toxicity evolution	Does not capture membrane retention, long SRT, sludge/EPS interactions, or continuous MBR operation

Continued on next page

Evidence category	Relative evidence strength	Typical evidence source	Relevance to MBR operation	Role in this review	Evidence boundary
Short-term material-performance evidence	Preliminary	Static adsorption tests, short-term membrane filtration, membrane-sheet antifouling tests, and independent antimicrobial experiments	Indicates material-level functional potential only	Used to identify possible adsorption, antifouling, catalytic, or antimicrobial functions	Short duration and simplified conditions; long-term MBR performance, metal release, fouling evolution, and resistance risk remain outside the test scope
Non-metal conductive reference evidence	Boundary/ reference	CNOs, conventional biochar, carbon-based conductive materials, and non-metal conductive interfaces	Not direct evidence for metal-based interfaces but relevant to conductive/electron-transfer mechanisms	Used only to illustrate EET enhancement, conductive-interface effects, or performance–risk decoupling	Supports conductive/electron-transfer mechanisms, not metal-specific effects or metal-driven resistance selection

*Note: The evidence hierarchy describes how directly each study type supports conclusions for continuously operated MBRs; it is not a ranking of methodological quality. The labels “High”, “Moderate to high”, “Supporting”, “Mechanistic/supporting”, “Preliminary”, and “Boundary/reference” indicate MBR-specific applicability.

In this review, we move from mechanism to risk and then to engineering relevance. In Section 2, we examine antibiotic removal and fouling control; in Section 3, we address metal-coupled electrochemical and bioelectrochemical interfaces and ARG responses; in Sections 4 and 5, we focus on spatial redistribution, co-selection, and dissemination within membrane biofilms and cake layers. In Section 6, we develop benefit–risk and safety-assessment criteria, and in Section 7, we identify the research questions that matter most for scale-up under realistic wastewater and long-term operating conditions.

2. Mechanisms by which metal-based functional interfaces enhance antibiotic removal and membrane fouling control in MBRs

2.1. Flocculation, bridging, co-precipitation, and EPS restructuring

Extracellular polymeric substances (EPS) connect sludge-floc structure, cake-layer development, and membrane fouling. Metal species such as Fe^{3+}, $Fe(OH)_3$, and Ca^{2+} interact with EPS functional groups through bridging, complexation, and precipitation, changing EPS conformation, floc structure, and cake-layer properties. In MBRs, these reactions occur across a bulk-liquid–EPS–sludge-floc–cake-layer continuum and directly reshape pollutant partitioning and fouling behavior. Table 3 compares the main mechanisms, study scales, strengths, and operating constraints of the interfaces discussed in this section.

Table 3. Comparison of mechanisms by which metal-based functional interfaces enhance antibiotic removal and membrane-fouling control.

Interface type	Representative materials/ systems	Scale of supporting studies	Antibiotic-removal mechanism	Fouling-control mechanism	Main advantages	Key constraints
Metal-ion conditioning	Fe^{3+}, Ca^{2+}	Bench-scale	Complexation, bridging, co-precipitation, and solid-phase partitioning	EPS reconstruction, larger flocs, and optimized cake-layer structure	Simple dosing and direct regulation	Narrow dosage window; excessive dosing can cause inorganic deposition
Iron-based particles	$Fe(OH)_3$, Fe_3O_4, nZVI	Bench-scale	Adsorption, Fe^{2+}/Fe^{3+} cycling, and reductive transformation	EPS/SMP regulation, floc conditioning, and loosening of cake layers	Potential synergy between removal and antifouling	Passivation, particle loss, and TP risks
Magnetic composites	Magnetic biochar and Fe_3O_4-biochar	Bench-scale	Adsorption-based enrichment, electron transfer, and co-metabolism	Improved sludge flocs and fouling layers	Recoverable and multifunctional interfaces	Long-term stability, recovery, and metal release remain poorly resolved
Metal-functionalized membranes	TA-Cu/PVDF and $Ag@SiO_2$	Bench-scale	Localized adsorption and antimicrobial, catalytic, or controlled-release effects	Greater hydrophilicity, weaker adhesion, and biofouling inhibition	Well-defined location of action	Continuous-operation evidence is narrow; chronic co-selection under metal release remains unresolved

Continued on next page

Interface type	Representative materials/systems	Scale of supporting studies	Antibiotic-removal mechanism	Fouling-control mechanism	Main advantages	Key constraints
Metal self-corrosion/ microelectrolysis interface	Fe^0-MABR and ZVI-AnMBR	Bench-scale	Fe^0 corrosion, iron cycling, and interfacial electron transfer	Biofilm-structure regulation and enhanced pollutant transformation	Potential to transform recalcitrant antibiotics	Iron-sludge accumulation, uncontrolled corrosion, and long-term maintenance
Metal-coupled electrochemical interface	eMBRs with metal electrodes or iron-based particles	Bench- to pilot-scale	Anodic/cathodic reactions, electron transfer, and reactive species	Electric-field regulation of EPS/SMP and membrane deposition	May increase transformation efficiency	Energy demand, side reactions, and limited ARG coverage

*Note: "Scale of supporting studies" refers to the principal MBR or membrane-coupled reactor evidence for each route. The literature remains dominated by bench-scale systems, with pilot-scale validation available for only a few configurations.

Fe^{3+} provides an example of metal-mediated floc regulation. In a laboratory MBR treating wastewater containing 1 mg/L sulfamethoxazole (SMX), 40 mg/L Fe^{3+} increased SMX removal from 53% to 70% and lowered the membrane-fouling rate from 2.52 to 1.03 kPa/d [17]. Adsorption, complexation, and co-precipitation of SMX by $Fe(OH)_x$ colloids or iron-hydroxo complexes can contribute to this response, together with Fe^{3+}-mediated EPS bridging. Fe^{3+} may also shift loosely bound EPS (LB-EPS) toward tightly bound EPS (TB-EPS), lowering the protein-to-polysaccharide ratio and the specific resistance of the cake layer. $Fe(OH)_3$ can adsorb soluble microbial products (SMP) and low-molecular-weight organics, incorporate fine colloids into larger flocs, and reduce fouling; a pharmaceutical-wastewater MBR showed an approximately 35% lower fouling rate after $Fe(OH)_3$ addition [27]. In practice, these interfaces change where pollutants reside as well as how the cake layer forms. A lower aqueous antibiotic concentration can reflect phase transfer, so it cannot be treated automatically as evidence of degradation.

Ca^{2+} shows why dosage matters. At an SRT of 15 d, approximately 280 mg/L Ca^{2+} increased membrane permeability by about 35%, whereas approximately 830 mg/L reduced it by about 50% relative to the control [28]. Lower Ca^{2+} levels can compact flocs through bridging; higher levels can intensify irreversible fouling through carbonate or phosphate precipitation. Cu^{2+} can also redirect tetracycline (TC) removal toward EPS-associated sorption sites [29], consistent with the abundance of functional groups and sorption domains in EPS [30]. Metal-mediated bridging has an operating window set by metal identity, dose, and the interfacial structure that develops in the reactor.

2.2. Redox and electron-transfer interfaces: Antibiotic transformation and operating dependence

Flocculation and co-precipitation mainly redistribute pollutants among phases. Redox-active materials such as nano-zero-valent iron (nZVI), Fe_3O_4, and magnetic biochar add another pathway by driving redox reactions and interfacial electron transfer. In the discussion below, we focus on when

these processes contribute to antibiotic transformation and where their performance boundaries appear.

nZVI is a representative iron-based redox interface. In an anaerobic membrane bioreactor (AnMBR) treating livestock wastewater, 2.6 g/L nZVI increased sulfonamide removal from 32%–62% to 64%–97% [23]. The response was strongly compound-specific: Sulfonamide removal improved, whereas removal of tetracycline, ciprofloxacin, and norfloxacin declined. Shifts in genera such as *Lentimicrobium* and *Methanomethylovorans* may contribute to these differences, although the study does not resolve a specific causal mechanism [23]. The result is useful precisely because it shows that nZVI performance cannot be generalized from one antibiotic class to another.

Fe_3O_4 also shows a strong location effect. After 40 d, TMP reached 41.9 kPa in R3-MBR, where nano-Fe_3O_4 was added only to sludge, compared with 62.7 kPa in the control R1-MBR. When Fe_3O_4 was added to sludge and the membrane surface in R4-MBR, fouling resistance fell by 46.08% relative to the control [31]. The relative abundance of Proteobacteria in R3-MBR rose from 25.06% to 45.11%, alongside broader changes in community structure [31]. Particle placement affects membrane behavior and the microbial environment around the interface.

Peanut-shell-derived magnetic biochar (MBC) improved AnMBR treatment of simulated pharmaceutical wastewater containing SMX, with 80% chemical oxygen demand (COD) removal and more than 90% SMX removal [24]. Several processes may contribute: Adsorption can enrich SMX near reactive or biological sites, conductive surfaces can stimulate direct interspecies electron transfer, and the material can support anaerobic microbial activity. MBC also reduced SMP from 22.2 to 6.3 mg/g volatile suspended solids (VSS), lowered EPS from 18.9 to 14.2 mg/g VSS, and increased sludge particle size from 60.6 to 113.4 μm, changes that can limit deposition of low-molecular-weight pollutants and fine flocs on the membrane [24]. Direct superiority over Fe_3O_4 cannot be claimed because the two materials have not been compared under identical AnMBR conditions. Liu et al. [25] further showed that MBC-mediated iron reduction, co-metabolism, and in situ SMX degradation can work together in a microbial electrochemical system. That study did not include membrane separation or membrane fouling, so it supports the transformation mechanism but does not establish MBR-scale performance.

Across nZVI, Fe_3O_4, and MBC systems, the recurring mechanisms are iron cycling, particle-surface reactions, adsorption-based enrichment, and microbial regulation. Their relative importance changes with material properties, dosing location, operating conditions, and antibiotic identity. nZVI can drive opposite responses for different compounds, while Fe_3O_4 antifouling performance depends on where it is introduced. MBC offers a multifunctional interface, but a head-to-head advantage over Fe_3O_4 has not been established. Engineering assessment needs to separate adsorption from transformation and track the formation and toxicity of TPs instead of relying on parent-antibiotic removal or fouling mitigation alone.

Table 4. Antibiotic-class-specific applicability, removal mechanisms, performance, and resistance risks of representative metal-based interfaces.

Antibiotic class	Representative antibiotics	Representative metal interface/system	Reported removal performance/effect	Dominant or proposed removal mechanism	Antibiotic-resistance risk	Practical implication
Sulfonamides	SMX and other sulfonamides	nZVI-AnMBR [23]	2.6 g L^{-1} nZVI increased removal from 32%–62% to 64%–97%	Enhanced biodegradation, iron-mediated redox processes, and microbial-community regulation	ARG/MGE responses were not directly quantified in this study	Among current MBR studies, sulfonamides show the clearest positive response to nZVI; direct resistance-risk data have not been reported
Sulfonamides	SMX	MEMBR [32]	SMX removal increased from 43.9% in MBBR to 88.9% in MEMBR	Electric-field effects, ROS generation by conductive carriers, and enhanced microbial transformation	ARG responses were not directly quantified	Strong removal enhancement; resistance response was outside the scope of the study
Sulfonamides	SMX	Fe^0 self-corrosion/ microelectrolysis-enhanced MABR [33]	SMX removal increased from approximately 47.8% to 93.3%	Fe^0 corrosion, iron-oxide adsorption/redox reactions, and microbial regulation	*sul1* and *sul2* decreased, with inhibition of their transfer to some extent	Provides relatively strong evidence for simultaneous antibiotic and selected ARG reduction
Tetracyclines	TC	nZVI-AnMBR [23]	nZVI reduced TC removal relative to the control AnMBR	Compound-dependent biodegradation and microbial-community responses; mechanism unresolved	Direct ARG responses were not reported	nZVI performance is compound-specific; tetracycline applications require separate validation

Continued on next page

Antibiotic class	Representative antibiotics	Representative metal interface/system	Reported removal performance/effect	Dominant or proposed removal mechanism	Antibiotic-resistance risk	Practical implication
Tetracyclines	CTC	AnEMBR [34]	At 45 mg L^{-1} CTC, 0.7 V maintained >86% CTC removal during the initial 15 d versus 60% under open circuit; removal decreased to 68% after 58 d	Electrochemical redox reactions and enrichment of CTC-degradation-related microbial functions	Total ARG abundance decreased in supernatant/effluent, but tetracycline-resistance genes increased by 130%–397%; ARGs/MGEs were strongly enriched in sludge	High removal efficiency may coexist with class-specific ARG enrichment and internal risk redistribution
Tetracyclines	TC	Ag^{+}/TC co-exposure [35]	Conventional treatment performance was not markedly impaired	Metal–antibiotic co-exposure, cellular stress, and membrane damage	*tetA*, *blaTEM-1*, and *sulII* increased substantially; evidence source: activated sludge, with no direct MBR validation	Ag-based interfaces need MBR-specific testing under residual tetracycline exposure
Fluoroquinolones	CIP, NOR	nZVI-AnMBR [23]	nZVI reduced CIP and NOR removal relative to the control AnMBR	Compound-dependent biodegradation and microbial-community responses	Direct ARG responses were not quantified	nZVI should not be generalized as a universal enhancer for fluoroquinolone removal
Fluoroquinolones	Multiple FQs	Pilot-scale EMBR [36]	Enhanced removal was observed for 3 fluoroquinolones relative to the conventional MBR	Direct anodic oxidation and ROS-mediated indirect oxidation	Class-specific ARG responses were not quantified	Electrochemical interfaces broaden the treatment range for fluoroquinolones; resistance response needs paired measurement
Macrolides	Multiple macrolides	Pilot-scale EMBR [36]	Enhanced removal was observed for 2 macrolides relative to the conventional MBR	Direct anodic oxidation and ROS-mediated indirect oxidation	Class-specific ARG responses were not quantified	Electrochemical treatment is promising for macrolides, but MBR-specific evidence remains sparse

Antibiotic class is another strong determinant of interface performance. Table 4 shows the most consistent enhancement for sulfonamides in nZVI- and electrochemical/microelectrolysis-based systems, while tetracyclines and fluoroquinolones respond more variably and can show poorer removal after nZVI addition. Electrochemical interfaces span a broader set of compounds because direct anodic oxidation and reactive-species-mediated pathways can act on sulfonamides, fluoroquinolones, and macrolides. Resistance responses do not necessarily follow removal performance. During CTC treatment in AnEMBRs, for example, parent-antibiotic removal improved while tetracycline-resistance genes became enriched. Selecting an interface for mixed-antibiotic wastewater requires compound-specific evidence on removal mechanism, achievable transformation, and resistance response.

2.3. Membrane-surface-functionalized metal interfaces: Antifouling performance and long-term evidence

Membrane-surface functionalization acts at a different point in the fouling process from metals added to mixed liquor. It changes the first contact between foulants and the membrane, influencing wettability, interfacial adhesion, microbial attachment, and localized antimicrobial or catalytic activity. Metal–polyphenol coordination layers can improve surface properties [21,37], and Ag-based layers can suppress biofouling through controlled metal release [38]. Tannic acid–iron membranes, metal-organic-framework active layers, and Co/Mn catalytic membranes have mostly been evaluated in nanofiltration, short-term separation, or stand-alone persulfate-activation systems [39–42], so they mainly provide mechanistic support for continuous MBRs; reactor-scale validation remains limited.

Continuous-MBR evidence is strongest for tannic acid–copper (TA-Cu) and Ag-based functionalized membranes. Maneewan et al. used a TA-Cu/polyvinylidene fluoride (PVDF) membrane in an AnMBR and obtained 91.8% ± 4.0% COD removal, close to the 92.2% ± 3.6% measured with the unmodified membrane [21]. The modification improved the interface without compromising conventional organic-matter removal. For an Ag@SiO_2 nanopollen-modified membrane, an Ag loading of 107.7 ± 10.9 μg/cm² and an Ag^+ release rate of about 0.5 μg/(cm²·d) produced a TMP-increase rate of 0.88 ± 0.34 kPa/d. The corresponding rates were 2.32 ± 0.86 kPa/d for the unmodified membrane and 2.25 ± 1.28 kPa/d for an Ag@SiO_2 membrane without the nanopollen structure [38]. No clear adverse effect on effluent quality, sludge activity, or microbial diversity was reported during 75 d of continuous operation [38].

The Ag@SiO_2 result supports a practical role for the SiO_2 shell in moderating Ag^+ release while maintaining surface antibiofouling. What it does not resolve is chronic selection. A 75-d operating period cannot establish whether prolonged exposure to low Ag^+ concentrations selects for ARGs, MRGs, or MGEs. Flux and TMP capture the operational benefit, but they do not close the environmental-safety question.

Membrane-surface metal functionalization has a clear advantage: It places the active interface exactly where initial deposition and biofilm formation begin. Continuous-MBR evidence is concentrated on TA-Cu and Ag-based membranes, while most other materials have been tested outside long-term membrane-coupled operation. Engineering evaluation should track functional-layer aging, metal release, resistance responses, and stability across repeated operating cycles. In Section 6.2, we develop these criteria in more detail.

3. Metal-coupled electrochemical and bioelectrochemical interfaces and ARG responses

3.1. eMBR/MEMBR: Antibiotic transformation under applied electric fields and spatial ARG responses

Electrochemical membrane bioreactors (eMBRs) and moving-bed electrochemical membrane bioreactors (MEMBRs) combine electrochemical reactions, microbial metabolism, and membrane separation through electrodes or conductive carriers. In the MEMBR developed by Chen et al., an applied electric field and carbon-felt particles created an electrochemical–biofilm composite interface. Low-concentration sulfamethoxazole (SMX) removal reached 88.9%, compared with 43.9% in a concurrently operated moving-bed biofilm reactor (MBBR), while the TMP-increase rate fell from 1.72 to 1.06 kPa/d [32]. Carbon-felt carriers may support reactive-oxygen-species generation, and the electric field increased microbial richness and diversity while enriching Actinobacteria and Gemmatimonadetes, taxa that may contribute to SMX mineralization [32]. The observed gain reflects the combined action of conductive carriers and the electric field, not the field in isolation.

Li et al. examined an anaerobic electrochemical membrane bioreactor (AnEMBR) treating chlortetracycline (CTC). Under open-circuit conditions at 45 mg/L CTC, 15 d of operation drove COD removal below 68%, CTC removal to 60%, and methane production to zero; supernatant and effluent turbidities rose to 40 and 30 NTU [34]. Applying 0.7 V changed that trajectory. During the first 15 d at the same CTC concentration, COD removal remained above 94%, CTC removal above 86%, and methane production showed no obvious inhibition. Performance weakened during longer exposure: After 58 d, COD and CTC removal were 72% and 68%, respectively, methane production was 27% below its initial level, and mean supernatant and effluent turbidities were 22 and 17 NTU, respectively [34]. The voltage delayed high-CTC stress but did not eliminate it.

ARG responses to the applied voltage were strongly compartment-specific. At 0.7 V, total relative ARG abundance in the supernatant and effluent fell by 71%–80% relative to the open-circuit high-CTC stage, and aminoglycoside-, MLSB-, and sulfonamide-resistance genes decreased by 77%–92%. Tetracycline-resistance genes moved in the opposite direction, increasing by 130%–397% together with enrichment of genes such as *tetX* [34]. Sludge showed a clearer divergence: total ARG and MGE abundances in anodic and cathodic sludge reached 57- and 150-fold the CTC-free control levels, respectively, above the corresponding 30- and 94-fold increases under open-circuit high-CTC conditions, respectively [34]. The voltage improved several aqueous-phase resistance indicators while shifting a substantial part of the resistance burden into the sludge phase.

eMBRs and MEMBRs can combine better antibiotic removal with slower fouling under suitable operating conditions. Their resistance outcome has to be read spatially. Effluent-relative abundance alone misses internal enrichment, so electrochemical-interface studies should quantify ARGs and MGEs across bulk liquid, sludge, electrode-associated biomass, and membrane-fouling layers.

3.2. MFC-MBRs and Fe^0-MABRs: ARG responses at bioelectrochemical and metal self-corrosion interfaces

Microbial fuel cell–membrane bioreactors (MFC-MBRs) and Fe^0-coupled membrane-aerated biofilm reactors (Fe^0-MABRs) provide two useful configurations for examining how

bioelectrochemical and metal self-corrosion interfaces affect antibiotics, fouling, and resistance. Direct evidence for simultaneous SMX and ARG/MGE reduction in MFC-MBRs comes mainly from one related series of studies [43–45] and centers on sul-type genes and *intI1*. That evidence is meaningful but narrow in wastewater type, reactor design, and target genes. Studies of MFCs and other bioelectrochemical systems add mechanistic support by linking antibiotic transformation, microbial-community shifts, and lower selection pressure to ARG responses [46–48]. These cross-system studies help explain possible pathways, but they do not carry the same weight as continuously operated MBR evidence.

Zang et al. developed an internally recirculated MFC-MBR with carbon felt as the anode and stainless-steel mesh as the cathode to treat synthetic wastewater containing 0.5 mg/L SMX. Relative to a conventional MBR, the system achieved higher SMX removal and substantially lower abundances of *intI1*, *sul1*, and *sul3* [43]. Internal recirculation likely increased mass exchange between mixed liquor and the anodic biofilm, while electroactive or electron-transfer-associated taxa such as *Geobacter* and *Desulfovibrio* were enriched. These changes can support bioelectrochemical SMX transformation and alter the host distribution of ARGs and MGEs [43,46,47]. Low-intensity bioelectricity may also reduce fouling by lowering EPS and SMP production, changing floc-surface properties, and reshaping membrane deposits [44,45].

Fe^0-MABRs use a different driving force: metal self-corrosion. Xue et al. coupled an Fe^0-packed bed with a membrane-aerated biofilm reactor to create a self-corrosion microelectrolysis-enhanced MABR. During stable treatment of 0.5 mg/L SMX, effluent concentrations were 260.93 ± 11.93 μg/L in the conventional S-MABR and 33.26 ± 3.66 μg/L in the Fe^0-enhanced S-eMABR, corresponding to an increase in removal from about 47.8% to 93.3% [33]. *sul1* and *sul2* also decreased, and their horizontal transfer was inhibited to some extent [33]. The combined evidence points to three linked effects of Fe^0 self-corrosion: lower antibiotic selection pressure, formation of iron-oxide adsorption/redox interfaces, and altered biofilm function.

The two systems should not be generalized beyond the conditions that produced those results. MFC-MBR performance depends on anodic-biofilm activity, internal recirculation, organic loading, antibiotic concentration, and cathode/membrane configuration. Fe^0-MABRs add further controls through corrosion rate, iron-oxide formation, biofilm thickness, and oxygen transfer. Decreases in *sul1*, *sul3*, or *intI1* establish responses for those indicators, not a system-wide decline across the resistome. The available studies also do not resolve whether stronger parent-antibiotic removal is accompanied by lower TP toxicity.

Carbon nano-onions (CNOs) provide a useful non-metal conductive reference. In an AnMBR, CNO addition reduced effluent chloramphenicol (CAP) to nearly undetectable levels during continuous operation; batch tests increased CAP removal from 59.4% to 90.4% within 10 h and lowered filtration resistance by about 11%; yet, *intI1* abundance increased [26]. This non-metal result is not direct evidence for risk decoupling at metal-based interfaces. However, it shows that stronger conductivity and extracellular electron transfer (EET) can improve treatment without lowering MGE-related risk. Metal-coupled electrochemical systems need compartment-resolved ARG/MGE measurements alongside parent-antibiotic removal and fouling data.

4. Membrane biofilms and cake layers as carriers of metal-based interfacial effects

4.1. Formation, temporal evolution, and spatial heterogeneity of membrane-fouling interfaces

Once metal-based materials enter an MBR, the active interface is continually rebuilt by EPS, SMP, inorganic salts, and microbial cells. Fe^{3+}, $Fe(OH)_3$, nZVI, Fe_3O_4, and magnetic biochar can complex, bridge, or adsorb onto EPS functional groups, producing composite interfaces that contain metal phases, EPS, and sludge flocs [49–52]. EPS is chemically diverse, with polysaccharides, proteins, lipids, nucleic acids, and other constituents that govern biofilm integrity, adsorption, and stress tolerance [49]. Extracellular DNA (eDNA) adds another layer: It supports adhesion and biofilm stability [53] and can chelate cations in ways that alter local antibiotic tolerance [54].

EPS and biofilm coverage can strengthen or weaken a metal interface depending on how the covering layer evolves. Greater local contact among antibiotics, eDNA, cells, and metal components can promote retention, transfer to solids, and microbial co-metabolism. The same layer can also mask reactive sites, slow mass transfer, hinder electron transfer, and accelerate aggregation or passivation of nZVI, Fe_3O_4, and magnetic biochar. Surface oxidation, oxide-shell formation, particle aggregation, and interfacial coverage are all known controls on nZVI and iron-oxide reactivity [50]. EPS further affects nanoparticle migration, accumulation, and reactivity through adsorption, encapsulation, complexation, and diffusion limitation [51,52]. Ag-nanoparticle studies in wastewater biofilms show a similar pattern: The EPS matrix changes actual microbial exposure and tolerance responses [55]. Long-term performance is governed by the interface that forms during operation; the material added at day zero is only the starting condition.

Membrane-fouling layers are spatially heterogeneous. AnMBR cake layers vary in physical structure, chemical composition, and microbial distribution [56], and full-scale MBR membrane biofilms can develop reproducible core communities that differ from random deposits of suspended sludge [57]. Layer-to-layer differences also appear in particle size, EPS protein structure, interfacial interaction energy, and microbial functional expression [58]. A useful conceptual picture is a continuum from bulk liquid to a loose outer cake and then to a denser inner membrane biofilm. Deposition, adsorption, bridging, and co-precipitation are often strongest in the outer region, while the inner region has denser EPS, longer local residence times, and stronger mass-transfer limitation [56,58]. The exact architecture varies among systems, but the spatial gradient is central to how metal interfaces behave.

Coverage has an especially direct effect on membrane-surface-functionalized interfaces. TA-Cu/PVDF membranes can delay early fouling by increasing hydrophilicity and weakening interfacial adhesion [21], while $Ag@SiO_2$ membranes can extend operating cycles through controlled Ag^+ release and reduced microbial attachment [38]. As cake layers and membrane biofilms mature, the functional layer becomes progressively screened from the bulk liquid and acts through the overlying deposit. Local pH, redox conditions, and coordination chemistry within that deposit can then feed back on metal speciation, migration, and bioavailability [51,52,55]. Membrane biofilms and cake layers are part of the functional interface itself, not merely material accumulated on top of it.

Time changes the interface as much as space does. Early behavior reflects the initial density of reactive sites, surface properties, and metal-release characteristics. During continued operation, EPS/biofilm coverage, particle aggregation, occupation of adsorption sites, and surface oxidation or

passivation can shift mass transfer, reactivity, and metal bioavailability [50–52]. Chemical cleaning adds another reset, but it is rarely a complete one: Foulants and microbial communities are removed or reorganized, while the post-cleaning physicochemical and biological state may differ from the initial membrane [59–61]. Repeated operation–fouling–cleaning–refouling cycles can move the system through different states of pollutant transformation, metal exposure, and ARG/MGE risk. Long-term studies need stage-resolved measurements across the operating cycle; a single end point misses that evolution.

4.2. Physical retention, spatial redistribution, and internal ARG enrichment

Membrane biofilms and cake layers retain and redistribute ARB, ARGs, MGEs, and eDNA. Membrane separation, particle retention, and adsorption within the fouling layer can lower intracellular and extracellular ARG release in the effluent [16,62,63], but retained genetic material remains inside the treatment train. It can shift from the bulk liquid into suspended sludge, loose cake, or dense membrane biofilms. This distinction matters because membranes and fouling layers act as barriers to release and as reservoirs that alter ARG partitioning [16]. Studies that separate intracellular and extracellular fractions have found markedly higher normalized abundances of target ARGs and *intI1* in fouling layers than in suspended sludge, while more severe fouling can lower the absolute abundance of extracellular ARGs in the effluent [64]. A cleaner effluent can coexist with a larger internal resistance reservoir.

EPS provides many of the binding sites that make this redistribution possible. Polysaccharides, proteins, and eDNA can retain antibiotics, metal components, and genetic material through adsorption, complexation, and encapsulation [49,53,54]. Metal-based materials further reshape the spatial pattern by changing EPS conformation, floc size, cake-layer pore structure, and membrane adhesion. Fe^{3+} and $Fe(OH)_3$ promote movement of antibiotics and fine particles into sludge or cake layers through bridging, flocculation, and co-precipitation [17,27]. Fe_3O_4 and magnetic biochar affect solid-phase partitioning and fouling structure through surface adsorption, iron redox cycling, and EPS/SMP regulation [25,31]. Once biofilm coverage develops on TA-Cu/PVDF or Ag@SiO_2 membranes, the metal layer also shifts from direct contact with the bulk liquid toward indirect control of attachment, retention, and metal exposure [21,38].

Fouling layers can also participate in antibiotic transformation. AnMBR studies have linked membrane-biofilm microbial activity to antibiotic transformation, giving these layers a biological function beyond simple retention [65]. In an AnMBR treating real levofloxacin-containing pharmaceutical wastewater, a moderately fouled membrane biofilm increased COD and levofloxacin removal by about 12% and 10%. Effluent *qnrA*, *qnrS*, and *intI1* absolute abundances were about 0.27 log units lower than during the low-fouling stage [66]. Under those conditions, adsorption, host retention, and biotransformation likely acted together to reduce pollutant and ARG release.

Better effluent indicators leave open what happened inside the reactor. Dense cell populations, abundant EPS/eDNA, and long retention in fouling layers can support persistence of ARG hosts and MGEs and create opportunities for genetic exchange [53,54,64,67]. Fouling layers have also shown higher ARG abundance and diversity than bulk sludge, consistent with their role as selective resistance reservoirs [68]. Three outcomes need to be separated: reduced release to the effluent, redistribution within the system, and genuine depletion of resistance-related genetic material. A meaningful risk

assessment should quantify absolute abundances and total loads of ARGs and MGEs in bulk liquid, suspended sludge, cake layers at different depths, membrane biofilms, and cleaning effluents, with intracellular and extracellular fractions resolved [63,64]. ARG diversity and potential hosts should be mapped across the same layers [58,68]. Substantive risk reduction requires a decline in the system-wide burden and mobility of resistance determinants. Transfer from water into retained biomass does not meet that criterion.

4.3. Three spatial coupling modes among metals, antibiotics, and ARGs in membrane-fouling layers

The relationships among antibiotic transformation, pollutant migration, and ARG/MGE responses can be organized into three coupling modes: synergistic reduction, enrichment and transfer, and risk decoupling (Figure 2). The classification draws on reactor-scale evidence for simultaneous antibiotic and resistance reduction [43–45,33], studies showing transformation within membrane-fouling layers [65,66], observations of internal ARG enrichment [64,68], and conductive-interface cases in which treatment performance and resistance indicators diverge [26]. These modes describe operating states at a given dose, stage, and location; they are not permanent labels attached to a material.

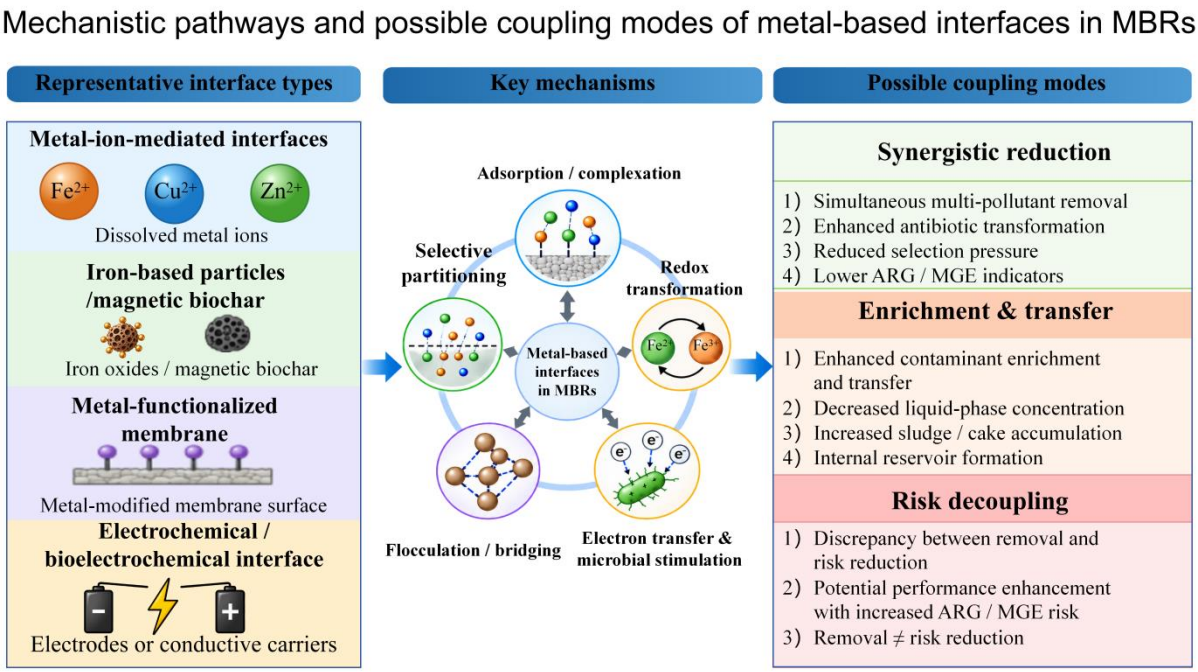


Figure 2. Key mechanisms and spatial coupling modes of metal-based functional interfaces in MBRs. Partitioning, adsorption, flocculation, redox reactions, and electron transfer can drive three system states: synergistic reduction, enrichment and transfer, or risk decoupling.

Synergistic reduction describes a state in which genuine antibiotic transformation increases, local selection pressure falls, and at least some ARG/MGE indicators decline at the same time. MFC-MBRs

and Fe^0-MABRs provide reactor-scale examples: stronger SMX removal occurred together with lower *intI1*, *sul1*, *sul2*, or *sul3* abundance [43–45,33]. Membrane-biofilm involvement in antibiotic transformation provides additional mechanistic support [65]. A moderately fouled AnMBR treating real pharmaceutical wastewater also improved levofloxacin removal while lowering effluent loads of *qnrA*, *qnrS*, and *intI1* [66]. These studies establish the mode under specific conditions, but they cover a limited set of reactors, wastewaters, and ARG subtypes and do not demonstrate a resistome-wide reduction in risk.

Enrichment and transfer occurs when lower aqueous antibiotic concentrations are driven mainly by adsorption, complexation, bridging, or co-precipitation, so pollutants move into sludge and fouling layers faster than they are transformed. Fe^{3+} and $Fe(OH)_3$ can drive this solid-phase transfer [17,27], while Fe_3O_4 and magnetic biochar change phase partitioning through adsorption, interfacial reactions, and EPS/SMP regulation [25,31]. Resistance determinants can concentrate in the same compartments: Normalized target ARG and *intI1* abundances may exceed those in suspended sludge, and fouling layers can carry greater ARG abundance and diversity [64,68]. Over time, adsorption-site saturation, surface oxidation or passivation, and EPS coverage can further reduce retention capacity or reactivity [50–52,55]. Because biofilms can support efficient gene transfer [67], retention-driven improvements should be treated as redistribution until transformation and system-wide risk reduction are demonstrated.

Risk decoupling describes the clearest mismatch between treatment performance and resistance outcome. CNO-enhanced AnMBRs, for example, improved CAP removal and lowered filtration resistance while *intI1* abundance increased [26]. CNOs are a non-metal reference, so this result does not establish the same response for metal interfaces. It does show that stronger conductivity and extracellular electron transfer can improve treatment without reducing MGE-related risk. Ag-containing interfaces raise a related question: EPS changes microbial exposure to Ag nanoparticles and associated tolerance responses [55], but chronic selection during long-term Cu/Ag release in MBRs has not been resolved. Short-term water quality, sludge activity, and community-diversity data are poor proxies for long-term ARG/MRG response.

The three coupling modes can shift during operation. Cake growth, EPS accumulation, particle aggregation, adsorption-site saturation, and surface oxidation or passivation progressively change retention, transformation capacity, metal bioavailability, and microbial exposure [50–52]. Cleaning then perturbs the system again by removing or reorganizing fouling layers and their microbial and chemical microenvironments [59–61]. A material that initially behaves in a synergistic-reduction state may later move toward risk decoupling or enrichment and transfer; some function may also recover after cleaning. Researchers mostly compare different reactors or isolated operating stages [58,64,68], so direct evidence of these temporal transitions within the same metal-based MBR is missing. Longitudinal sampling across start-up, mature fouling, post-cleaning, and refouling stages should track parent antibiotics and TPs, metal speciation, ARGs/MGEs, and interfacial properties together.

Operational classification needs a small set of diagnostics that can be measured consistently. Four dimensions are sufficient to separate the three modes conceptually: genuine antibiotic transformation, solid-phase accumulation of parent compounds and TPs, system-wide absolute ARG/MGE loads, and dissemination potential. Universal numerical thresholds are not available across MBR configurations, materials, antibiotics, and analytical platforms, so directional changes relative to a matched control or baseline are better suited to the available evidence than fixed cutoffs. Synergistic reduction requires

stronger genuine transformation together with a lower total ARG/MGE burden and no increase in dissemination indicators. Enrichment and transfer applies when aqueous concentrations fall mainly because pollutants are retained in sludge, cake layers, or biofilms while system-wide pollutant or resistance loads do not decline. Risk decoupling applies when removal or fouling control improves but ARG/MGE burden or dissemination potential remains unchanged or rises. Conflicting indicators should be reported as a transitional or mixed state.

A complete assessment should pair parent antibiotics and TPs with metal speciation and spatial distribution, absolute ARG/MGE abundances, potential hosts, and mobility [58,63,64,68]. Cu^{2+}, Zn^{2+}, and Ag^{+} can sustain selection pressure even when parent-antibiotic concentrations have fallen [69–71]. Membrane biofilms and cake layers occupy a pivotal position: They are major sites of pollutant retention and transformation, yet they can become microenvironments in which antibiotics, metals, and resistance determinants co-accumulate. Assigning a coupling mode from effluent antibiotic concentration or membrane performance alone would miss that internal state.

5. Mechanisms linking metal-based functional interfaces to ARG co-selection risk

5.1. Co-resistance: Retention and selection of ARG–MRG co-carriers in MBR solids

Co-resistance arises when antibiotic resistance genes (ARGs) and metal resistance genes (MRGs) occupy the same host cell, plasmid, transposon, integron, or other mobile genetic unit [70,72,73]. Under sustained Cu^{2+}, Zn^{2+}, or Ag^{+} exposure, hosts or mobile elements carrying the corresponding MRGs can gain a selective advantage [69–71]. When ARGs are physically linked to those MRGs, the same selection can maintain both resistance traits [72,73]. Plasmid metagenomes from wastewater treatment plants contain multiple ARGs and MRGs, and complete circular plasmids carrying resistance genes have been assembled, confirming plasmids as important vehicles for co-retention and dissemination [74]. Evidence for co-resistance rests on physical linkage and persistence under metal pressure, not on abundance correlations alone.

Membrane separation can lower effluent loads of ARGs and resistant hosts [75,76], but the retained genetic material remains within the biological process. Some ARGs and *intI1* occur at higher normalized abundance in membrane-fouling layers than in suspended sludge [64], and ARGs are widespread in activated sludge from large-scale MBRs [77]. SRT and mixed liquor suspended solids (MLSS) further control how long potential co-resistance carriers remain in the system. In a sequencing-batch MBR treating livestock wastewater, ARG copy-number removal reached 2.91 log at an SRT of 12 d. Extending the SRT to 30 d reduced biological ARG-removal capacity and increased ARG and MGE abundance inside the reactor, even though the membrane continued to restrict their effluent release [78]. Longer retention can increase residence time for tolerant hosts and mobile carriers as well as provide more time for treatment.

Dense biofilms increase cell-to-cell contact and can favor plasmid conjugation and other horizontal gene-transfer processes [79–82]. In one MBR study, the RP4 plasmid transferred from donor bacteria to culturable activated-sludge bacteria at an average frequency of 2.76×10^{-5} per recipient, while its abundance in total DNA remained near 10^4 copies/mg biosolids [83]. This result establishes that MBR environments can support transfer and persistence of mobile genetic carriers. Metal stress

was outside the experiment, so the finding defines the transfer capacity of the MBR environment itself and leaves metal-driven co-resistance as a separate question.

When Cu, Zn, or Ag accumulates in sludge flocs and membrane-fouling layers, membrane retention can combine with metal selection. Hosts carrying MRGs may be favored, and ARGs physically linked to those MRGs on plasmids, integrons, or other MGEs can persist even after parent-antibiotic concentrations fall [73,84,85]. Fe^{3+} and $Fe(OH)_3$ require a different interpretation because their main documented roles are flocculation, bridging, and solid-phase transfer. Any co-selection pressure from iron will depend on speciation, bioavailable concentration, and exposure time; total iron concentration alone is not an adequate proxy.

The decisive question for co-resistance in a metal-based MBR is whether retained ARGs and MRGs occupy the same hosts or mobile carriers and whether those co-carriers gain a selective advantage under metal exposure. Long-read metagenomics, plasmidomics, metagenomic Hi-C, and single-cell association approaches can resolve these physical linkages. Experiments that vary metal dose, SRT, and sludge-wasting rate are also needed to separate passive membrane retention from active enrichment driven by selection.

5.2. Cross-resistance: Efflux systems, EPS barriers, and shared tolerance in membrane-fouling layers

Cross-resistance describes shared physiological or functional mechanisms that reduce microbial sensitivity to metals and antibiotics. Physical co-localization of ARGs and MRGs is not required. Relevant mechanisms include efflux transport, cell-envelope regulation, oxidative-stress defense, and extracellular sequestration [73,84]. In the literature reviewed here, direct MBR evidence mainly captures reactor-scale ARG/MGE and community responses. Efflux- and EPS-mediated shared tolerance within membrane biofilms or cake layers is supported more strongly by mechanistic studies from related systems, so the pathway is plausible but not resolved at layer scale in MBRs.

Efflux is one route to cross-resistance, but metal-specific pumps and broad-spectrum antibiotic-efflux systems should not be conflated. RND-family multidrug pumps can lower intracellular concentrations of several antibiotics [86]. CzcCBA, by comparison, primarily exports Co^{2+}, Zn^{2+}, and Cd^{2+}, while CusCFBA/CusCBA mainly handles Cu(I) and Ag(I) [87]. Links between metal-specific efflux and antibiotic tolerance can emerge through transport-network interactions, cell-envelope stress, or selection of tolerant hosts even when the pump does not directly export the antibiotic [86,87]. River biofilms co-exposed to Cu^{2+} and enrofloxacin showed shifts in resistance phenotypes and resistance-gene composition, with multidrug efflux implicated as one component of shared tolerance [88]. That study offers cross-system mechanistic support; direct evidence from MBR fouling layers is absent. Increases in *czc*, *cus*, *cop*, or broad-spectrum efflux genes are most informative when paired with expression data, intracellular pollutant concentrations, and tolerance phenotypes.

The long SRT and high MLSS typical of MBRs extend the time available for degradation and microbial adaptation. This is a genuine trade-off. Longer retention can support antibiotic biodegradation and can prolong the residence of tolerant hosts and mobile genetic carriers; a sequencing-batch MBR treating livestock wastewater showed that increasing SRT did not produce a monotonic reduction in ARG/MGE risk [78]. High cell density and restricted diffusion within biofilms add further opportunities for close microbial contact and shared tolerance [79,89].

EPS may provide the spatial matrix in which this shared tolerance develops. In membrane biofilms and cake layers, EPS can adsorb or complex metal ions and retain antibiotics, TPs, and eDNA, changing the rate at which these stressors reach cells [49,79]. Under Zn(II) stress in bioreactors containing multiple antibiotics, increased protein release into EPS created binding sites that interacted with Zn(II) and antibiotics through metal coordination, hydrogen bonding, hydrophobic interactions, and salt bridges [90]. The mechanism can buffer acute toxicity, although its importance within specific MBR fouling-layer depths needs direct measurement.

EPS buffering can lower acute exposure while prolonging subinhibitory contact. In activated-sludge reactors co-exposed to environmentally relevant Ag^+ and tetracycline, conventional treatment performance changed little, yet cellular respiration, membrane structure, and permeability were altered, and effluent *tetA*, *blaTEM-1*, and *sulII* increased significantly [35]. Stable COD or other routine water-quality indicators can coexist with cell-level stress and resistance selection. This is particularly relevant to Ag-functionalized membranes, where slowly released metal and residual antibiotics may act together. Moreover, whether EPS reduces selection depends on bioavailability: Strong adsorption, complexation, or encapsulation can lower effective exposure, while delayed diffusion without stable immobilization or degradation can extend subinhibitory exposure. An MBR study showed concentration-dependent microbial-community and ARG responses to antibiotics [91], but it did not directly resolve efflux activity, EPS protection, or local selection pressure inside membrane biofilms.

Cross-resistance may appear in function before it appears in ARG copy number. Candidate signals include higher efflux-pump expression, activation of metal-homeostasis systems, altered membrane permeability, increased EPS secretion, stronger oxidative-stress defenses, and enrichment of tolerant taxa [86,87,90,35]. Combining transcriptomics and proteomics with efflux-pump inhibition, intracellular metal/antibiotic measurements, and tolerance assays would help distinguish direct cross-efflux from broader stress adaptation and community replacement.

5.3. Co-regulation: Stress responses and MGE activation across membrane-biofilm gradients

Co-regulation operates at the level of gene expression and signaling. Metal stress can activate regulatory networks that affect metal homeostasis, antibiotic tolerance, oxidative stress, and MGE activity at the same time. CueR, ZntR, ArsR/SmtB, and MerR are among the systems involved in metal homeostasis and toxicity buffering [87,92]. The class 1 integron-integrase gene *intI1* is widely used as an indicator of anthropogenic pollution and integron-associated resistance potential [93], and the SOS response can directly control integron recombination [94]. Heavy-metal stress in activated sludge has also been associated with oxidative-stress responses and higher plasmid-transfer frequency [95]. These observations define a plausible regulatory route from metal exposure to MGE activity, although the complete chain has not been demonstrated in metal-based MBRs.

MBR operation can amplify the opportunity for co-regulatory responses by extending exposure time and host contact. Membrane retention and long SRTs prolong the residence of resistant hosts and mobile genetic carriers [78], while biofilm growth increases local cell density and cell-to-cell contact [79,82]. RP4 transfer and persistence in MBRs show that this environment can sustain mobile genetic carriers [83]; this experiment established the transfer capacity of the MBR environment. It did not include metal stress, so metal-enhanced transfer remains untested in that study.

Activated-sludge experiments provide the clearest reactor-scale evidence for metal-stress effects on dissemination. Under Pb, As, and Hg exposure, resistance-plasmid transfer frequency increased by 1.7–3.6-fold, while expression of outer-membrane-protein-related genes rose by 2.9–7.4-fold and oxidative-stress-regulatory genes by 7.8–13.1-fold relative to the control [95]. The pattern links metal stress with cell-envelope responses, oxidative stress, and greater transfer potential. Because the researchers used sequencing-batch reactors without membrane retention or membrane-biofilm gradients, their results support the mechanism but do not define the magnitude of the effect in MBRs.

Spatial gradients within membrane-fouling layers add another level of control. EPS composition, particle structure, mass transfer, and microbial function vary with depth [58], so metal exposure and cellular stress are unlikely to be uniform across the layer. Direct MBR evidence for layer-specific co-regulation is absent. Stratified measurements of metal-homeostasis genes, oxidative-stress responses, SOS activity, and integrase expression would show whether the regulatory signal is concentrated in particular fouling-layer zones.

Three-dimensional biofilm-electrode reactors illustrate how such spatial responses can emerge. Under co-exposure to sulfadiazine, ciprofloxacin, and Zn, electrical stimulation improved pollutant removal while enriching some ARGs in electrode biofilms and lowering their abundance in the effluent [96]. The treatment benefit coincided with internal redistribution of resistance determinants. Zn(II)-stress studies have also reported concurrent increases in Zn-resistance genes, tetracycline ARGs, and MGEs, with some MGEs acting as potential bridges in ARG–MRG association networks [90]. Co-regulation and co-resistance can operate together: One changes expression and stress state, while the other selects or retains genetic carriers containing multiple resistance determinants. Separating the concepts helps identify the dominant mechanism even when both are present in the same fouling layer.

For TA-Cu and Ag@SiO_2 membranes, effective microbial exposure after biofilm formation depends on metal release, EPS complexation, and local diffusion [21,38]. No continuous-MBR study reviewed here measured metal concentration, stress-gene expression, and MGE activity across fouling-layer depth in the same experiment. Metal-homeostasis, oxidative-stress, efflux, or integrase activation cannot be inferred from metal-release rates or membrane operating cycles alone. ARG and *intI1* enrichment in fouling layers adds to that uncertainty [64]. Gene abundance shows that a genetic unit is present and accumulating; regulatory activation requires expression or functional evidence. Increases in *intI1*, SOS-gene expression, mobilizable circular intermediates, or plasmid-conjugation frequency can reveal greater dissemination potential even when the ARG copy number barely changes [81,82,93,94].

A convincing test of co-regulation needs to go beyond endpoint qPCR. Metal-homeostasis and oxidative-stress expression [87,92], SOS and integrase responses [93,94], plasmid conjugation, integron-gene-cassette rearrangement, and mobilizable circular intermediates should be measured together [81,82]. Layer-resolved transcriptomics would add the spatial information that bulk samples miss. The pieces of the mechanism already exist in separate datasets: MBRs can retain mobile plasmids [83], metal stress can increase plasmid transfer and stress responses [95], and biofilm-electrode systems can redistribute ARGs and MGEs [96]. What remains unresolved is the full sequence from local metal exposure to regulatory activation, MGE activation, and actual ARG dissemination inside a metal-based MBR. MBR-specific features can push the system in either direction. Long SRT, high MLSS, membrane retention, and dense biofilms can prolong host residence and cell contact [78,79,82], while

EPS adsorption and complexation can lower the freely bioavailable metal fraction [49,79,90]. The same EPS barrier may also extend subinhibitory exposure if retained contaminants are not transformed. Cross-system evidence is used here to define mechanisms; the direction and magnitude of those mechanisms must be resolved under MBR operating conditions.

Table 5 compares ARG/MGE responses, proposed mechanisms, evidence type, and risk interpretation across representative systems. The consistent message is that stronger antibiotic removal or slower fouling does not guarantee a lower resistance burden. Benefit–risk assessment has to track performance and where resistance determinants end up.

Table 5. Evidence comparison for ARG/MGE responses to metal-based and metal-coupled interfaces.

Interface/system	Target pollutant	ARG/MGE response	Potential mechanism	Evidence type	Interpretation
MFC-MBR	SMX	Decreases in *intI1*, *sul1*, and *sul3*	Bioelectrochemical transformation, lower selection pressure, and host changes	Direct evidence from continuous MBR operation	Synergistic-reduction signal for selected ARGs; broader resistome coverage is needed
Fe^0-MABR	SMX	Downregulation of *sul1* and *sul2*	Fe^0 corrosion, iron cycling, and reduced antibiotic-selection pressure	Direct evidence from a membrane-coupled reactor	Supports simultaneous SMX and selected sul-gene reduction; TP and durability data are absent
AnEMBR/eMBR	CTC or PPCPs	Lower relative ARG abundance in supernatant/effluent	Electric-field-enhanced antibiotic transformation and altered microbial metabolism	Direct or semi-direct evidence	Aqueous-phase decrease; absolute loads, hosts, and sludge/fouling-layer distribution remain to be resolved
Ag+/TC activated-sludge system	TC	Increases in *tetA*, *blaTEM-1*, and *sulII*	Joint metal-antibiotic stress and altered cell membranes	Non-MBR risk reference	Supports long-term co-selection testing for Ag-based membranes
CNO-AnMBR	CAP	Increase in *intI1*	Decoupling between EET enhancement and MGE responses	Non-metal conductive reference	Clear example of performance–risk decoupling at a conductive interface
Three-dimensional biofilm-electrode reactor	SDZ, CIP, and Zn	Some ARGs enriched in electrode biofilms while effluent abundance decreases	Spatial redistribution, electrical stimulation, and metal co-exposure	Related biofilm-electrode evidence	Separates lower effluent release from internal biofilm enrichment
Metal-stressed SBR	Pb, As, and Hg	Increased plasmid-transfer frequency	Oxidative stress, altered membrane permeability, and MGE activation	Non-MBR supporting evidence	Supports a mechanism by which metal stress can raise dissemination potential

6. Benefit–risk boundaries and safety assessment for metal-based functional interfaces in MBRs

6.1. Benefit–risk profiles of different technical routes

The benefit–risk profile of a metal-based functional interface is set by metal identity, material form, location of action, reactor configuration, and operating conditions. The evidence reviewed here falls into three broad technical routes: Iron-based strategies, Cu/Ag-based membrane-surface functionalization, and conductive or bioelectrochemical systems. These routes are not directly interchangeable because they differ in mechanism, study scale, and the endpoints used to judge performance. In the comparison below, we focus on what each route can support, where the main risks arise, and which evidence gaps matter for engineering decisions.

Among the routes reviewed here, iron-based strategies have the broadest direct MBR evidence for improving antibiotic removal and membrane performance. Fe^{3+}, $Fe(OH)_3$, Fe_3O_4, nZVI, and magnetic biochar act through different combinations of flocculation, adsorption, iron redox cycling, electron transfer, and microbial regulation [17,23,24,27,31]. Their value lies in this mechanistic range: Some interfaces primarily reorganize flocs and cake layers, while others add redox or electron-transfer functions. Most supporting studies remain laboratory-scale and focus on specific antibiotics over limited operating periods [23,24,31]. The next question for this route is durability: Whether the same performance persists as particles age, surfaces passivate, and fouling layers evolve.

The resistance and environmental-risk side of iron-based strategies is much less resolved than their treatment performance. Four testable pathways emerge from the available MBR and cross-system evidence. Fe^{3+}/$Fe(OH)_3$ flocculation, adsorption, and co-precipitation can move residual antibiotics from water into sludge and fouling layers [17,27]; incomplete transformation would leave selection pressure concentrated in high-biomass compartments. nZVI and Fe_3O_4 can accumulate in the same regions and lose reactivity through aggregation, oxidation, passivation, and EPS coverage [50–52], potentially shifting an interface from transformation toward retention as it ages. Iron-mediated redox and catalytic reactions can also generate TPs with toxicity profiles that differ from the parent compounds; non-MBR reaction systems show dynamic TP formation and toxicity evolution [97–99]. Finally, long-term co-retention of iron particles, residual antibiotics, and resistant hosts may create local conditions that favor ARG/MGE persistence or enrichment, although direct evidence for iron-driven resistance selection in MBRs is not available [64,68]. These are risk hypotheses, not established adverse outcomes. Testing them requires iron speciation and mass balances together with layer-resolved measurements of antibiotics, TPs, absolute ARG/MRG/MGE loads, hosts, and dissemination indicators across long-term operation and cleaning cycles.

Cu/Ag-based membrane functionalization has a different strength: The active material is localized at the membrane surface, where it can directly alter wettability, adhesion, and microbial attachment. TA-Cu/PVDF and Ag@SiO_2 membranes have shown antifouling benefits during continuous MBR operation [21,38], but the evidence base is small in material diversity and operating duration. The central risk is chronic selection from Cu or Ag, especially when MRGs and ARGs share plasmids, integrons, or other MGEs [73,74]. EPS can modify microbial exposure to Ag nanoparticles, and Ag^+ co-exposure with antibiotics has promoted selected ARGs in activated sludge [55,35]. Those observations come mainly from biofilm, plasmid-metagenomic, and activated-sludge studies.

Continuous MBR studies have yet to resolve ARG–MRG co-localization, MGE activation, or long-term host succession under sustained membrane-derived metal release. These studies establish antifouling potential; the co-selection boundary needs to be measured in the same membrane-coupled systems.

Conductive and bioelectrochemical systems can increase antibiotic transformation through electric fields, electrodes, conductive carriers, and in some cases iron-based self-corrosion. MEMBRs and eMBRs have improved removal of SMX and other pharmaceuticals, while AnEMBRs can buffer high-concentration CTC stress and lower several aqueous-phase ARG indicators [32,34,36]. MFC-MBRs have combined stronger SMX removal with lower *intI1*, *sul1*, and *sul3*, and Fe^0-MABRs have shown a similar pattern for SMX, *sul1*, and *sul2* [43,33]. The evidence is promising but clustered around a small number of reactor configurations, synthetic wastewaters, and target genes. Other systems show why a broader risk view is needed: CNO-enhanced AnMBRs increased *intI1* despite better CAP removal, while three-dimensional biofilm-electrode reactors shifted some ARGs into electrode biofilms as effluent abundance fell [26,96]. Electrochemical operation also introduces energy demand, electrode wear, and side reactions [100], while treatment can alter TP pathways and toxicity [98]. The outcome depends on the operating window as much as on the reactor type.

Engineering value also depends on the extra energy and material burden created by electrochemical integration. Conventional MBRs typically consume about 0.4–0.8 kWh m^{-3}, while electrochemical demand varies with current density, electrode material, aeration, operating mode, and scale [100]. Representative eMBR studies report around 0.6 kWh m^{-3} together with measurable sacrificial-anode consumption; increasing current or charge loading can accelerate electrode corrosion and raise replacement and maintenance needs. Removal gains and fouling control are meaningful only when energy input, electrode durability, and operating cost remain acceptable. Comparable pilot- and full-scale techno-economic datasets are too sparse for a robust ranking of eMBRs, MEMBRs, and MFC-MBRs.

The three routes occupy different parts of the benefit–risk space. Iron-based strategies have the broadest treatment-performance evidence but relatively little long-term resistance-risk data. Cu/Ag membrane functionalization offers localized antifouling control, while continuous-operation and co-selection datasets remain narrow [21,38]. Conductive and bioelectrochemical systems can couple removal with fouling control, but internal ARG/MGE redistribution remains an active constraint [26,96], alongside energy demand and electrode-related side reactions [100]. A fair comparison should use genuine antibiotic transformation, membrane stability, TP toxicity, metal release, total ARG/MGE burden, dissemination potential, and engineering cost; effluent concentration and TMP are only two parts of that picture. In Section 6.2, we translate these dimensions into an assessment framework.

6.2. System-level safety-assessment framework

Pollutant assessment needs to separate disappearance from transformation. For interfaces dominated by flocculation, adsorption, or co-precipitation, antibiotic mass should be tracked across bulk liquid, sludge, and membrane-fouling layers so that solid-phase transfer is not counted as degradation. Table 6 shows a recurring gap in direct MBR studies: nZVI, Fe_3O_4, MEMBR, AnEMBR, and related electrochemical systems often report parent-antibiotic removal, but individual TPs, absolute TP concentrations, and toxicity trajectories are rarely measured together [23,31,32,34,36].

nZVI-assisted AnMBR treatment, for example, substantially increased sulfonamide removal without resolving the identities or concentrations of the products formed [23]. Electrochemical MBR studies similarly attribute removal to electrochemical reactions, reactive species, and enhanced microbial processes without closing TP-resolved mass balances [32,34,36]. Non-MBR reaction studies fill part of that mechanistic gap: Iron-based and electrochemical oxidation can generate multiple intermediates, and toxicity can decline steadily or rise transiently before later detoxification [97–99]. A pollutant-level safety claim requires mass balance, transformation pathways, TP concentrations, and residual toxicity in addition to parent-compound removal.

Operational assessment should track membrane performance and metal behavior in the same time frame. Relevant membrane metrics include TMP, flux, permeability, reversible and irreversible fouling resistance, EPS/SMP composition, and cake-layer structure [15,19,20]. Metal measurements should cover dissolved fractions, chemical speciation, leaching, particle loss, and accumulation in sludge and fouling layers. These quantities can change as particles aggregate, surfaces passivate, EPS covers reactive sites, or functional layers deteriorate [50–52]. Cleaning interval or short-term flux recovery provides only part of the operating picture. Repeated measurements at start-up, mature fouling, immediately after chemical cleaning, and during refouling can reveal whether interface activity and resistance response recover, deteriorate, or show hysteresis over successive cycles.

Quantitative metal-fate data are much thinner than performance data. Most researchers report the initial dose, membrane loading, or a release metric, with little compartment-resolved recovery. Fe^{3+} was dosed at 40 mg/L in a laboratory MBR [17], and nZVI at 2.6 g/L in an AnMBR [23], but the summarized evidence does not close the Fe balance across liquid, sludge, cake, and membrane-associated phases. The Fe_3O_4 study compared addition to sludge and/or the membrane surface [31] without establishing system-wide particle recovery. TA-Cu/PVDF operation used a TA:Cu(II) molar ratio of 1:3 [21]; yet, quantitative Cu release and reactor-wide partitioning were not resolved. Ag@SiO_2 provides the clearest release metric, with 107.7 ± 10.9 μg Ag/cm² loaded on the membrane and Ag^+ released at about 0.5 μg/(cm²·d) [38], but even this study did not close a system-wide Ag balance across suspended sludge, cake/biofilm, effluent, and cleaning streams. Table 7 separates these input or release measurements from true phase-resolved mass balances.

Table 6. Transformation-product evidence and toxicity evolution for representative iron-based and electrochemical antibiotic-treatment interfaces.

Interface/system	Antibiotic	Experimental condition / concentration	Major TPs or transformation information	TP concentration/ abundance	Toxicity evolution	Evidence type
nZVI-AnMBR [23]	Tetracyclines, fluoroquinolones, sulfonamides	2.6 g L^{-1} nZVI	TP identities were not determined; enhanced sulfonamide removal was attributed mainly to improved biodegradation	Not reported	Not evaluated	Direct MBR evidence
Fe_3O_4-MBR [31]	No specific antibiotic targeted	Nano-Fe_3O_4 added to sludge and/or membrane surface	Antibiotic-specific TPs were not investigated	Not reported	Not evaluated	Direct MBR evidence; TP gap
MEMBR [32]	SMX	Low-concentration SMX (ng L^{-1}–μg L^{-1} range)	ROS generation and microbial processes were proposed; individual TPs were not identified	Not reported	Not evaluated	Direct MBR evidence
AnEMBR [34]	CTC	2.5–45 mg L^{-1} CTC	Enhanced CTC removal and enrichment of *tetX* were observed, but individual TPs were not resolved	Not reported	Not evaluated	Direct MBR evidence
Pilot EMBR [36]	Fluoroquinolones, macrolides, sulfonamides and other PPCPs	Real municipal wastewater	Direct anodic and ROS-mediated oxidation proposed; individual antibiotic TPs were not systematically quantified	Not reported	Not evaluated	Pilot-scale MBR evidence
nZVI batch system [101]	SMX	nZVI/SMX mass ratios 1:1–25:1	Five TPs detected at m/z 156, 192, 256, 294 and 296; redox transformation dominated over adsorption	Absolute TP concentrations not reported	Not evaluated in this study	Non-MBR mechanistic evidence
Modified nZVI (nZVI–β-CDP) [102]	SMX	>95% degradation within 10 min	SMX reduction products were detected	Not quantitatively resolved	Degradation products were less toxic than parent SMX toward *E. coli* and *R. subcapitata*	Non-MBR mechanistic evidence

Continued on next page

Interface/system	Antibiotic	Experimental condition / concentration	Major TPs or transformation information	TP concentration/ abundance	Toxicity evolution	Evidence type
Fe_3O_4/PS [103]	TC	41.6 μM TC; 1 g L^{-1} Fe_3O_4; 1 mM PS	Six major TPs: m/z 344, 358, 274, 290, 256 and 284	TP1–TP5 initially accumulated and subsequently decreased; TP6 increased during treatment; absolute concentrations not reported	Not evaluated	Non-MBR mechanistic evidence
Ultrasound/Fe_3O_4-Fenton [104]	TC	Heterogeneous Fenton-like oxidation	Oxidative intermediates generated during incomplete mineralization	Not systematically quantified	Toxicity initially increased and subsequently decreased during prolonged oxidation	Non-MBR mechanistic evidence
Electro-Fenton [98]	SMX	Initial SMX ≈0.21 mM	Cyclic/aromatic intermediates followed by short-chain carboxylic acids	Major carboxylic acids reached approximately 0.1–0.3 mM	Toxicity varied non-monotonically with electrolysis time and current because TPs formed and subsequently disappeared	Non-MBR mechanistic evidence
BDD electrochemical oxidation [105]	SMX	Electrochemical oxidation at 30 mA cm^{-2}	Hydroxyl substitution, oxidation of $–NH_2$ to $–NO_2$, and hydroxylation of the isoxazole ring	Individual TP concentrations not reported	*E. coli* inhibition decreased from 22.8% initially to 10% after 2 h and nearly zero after 4 h	Non-MBR mechanistic evidence

Resistance-risk assessment should move from single genes toward the architecture of resistance in the whole system. Useful endpoints include absolute ARG abundance, intracellular and extracellular fractions, MRGs, *intI1*, potential hosts, ARG–MRG co-localization, and linkage to plasmids, integrons, and transposons [69–73,84,85,106,107]. Lower effluent ARG abundance can result from membrane retention or solid-phase enrichment, as shown in Sections 4.2 and 5.1 [64,68]. Systems with controlled metal release, electric fields, or long-term subinhibitory exposure should also measure SOS/integrase responses, efflux systems, and metal-homeostasis or oxidative-stress genes when co-regulation or MGE activation is part of the proposed mechanism [87,92,94,95].

Spatial resolution is essential because the same interface can produce opposite signals in different compartments. Sampling should extend from influent and effluent to bulk liquid, suspended sludge, cake layers, membrane biofilms, and cleaning effluents. Layer-resolved concentrations and mass loads can distinguish genuine removal from liquid-to-solid transfer and internal enrichment of resistance determinants [16,58,64]. Conductive and bioelectrochemical systems need an additional compartment: electrode biofilms. ARGs and MGEs should be quantified separately there because electrical interfaces can lower effluent release while concentrating some genetic material inside attached biofilms [96].

An integrated safety assessment should bring seven endpoints into the same frame: genuine degradation, TP toxicity, membrane stability, net metal release, total ARG/MGE burden, potential hosts, and dissemination potential. Table 8 organizes these indicators by assessment level and priority. The practical shift is simple: Judging a metal-based interface from effluent antibiotic concentration or TMP alone is no longer enough once metals, retained biomass, and resistance determinants are interacting inside the reactor.

Table 7. Quantitative metal-input, release, and phase-resolved fate evidence for representative metal-based interfaces in MBRs.

Metal/interface	Representative MBR system	Reported dose/loading	Dissolved/released metal	Sludge/cake/biofilm evidence	Phase-resolved mass balance	What remains unresolved
Fe^{3+} conditioning [17]	Laboratory MBR treating 1 mg/L SMX	40 mg/L Fe^{3+}	NR	Quantitative Fe recovery in sludge/cake: NR	No	Dose quantified; phase-resolved Fe distribution not established.
nZVI [23]	AnMBR treating swine wastewater	2.6 g/L nZVI	Fe^0/Fe^{2+}/Fe^{3+} fractions: NR	Quantitative Fe recovery in biosolids/fouling layer: NR	No	Dose quantified; Fe speciation and compartmental recovery unresolved.
nano-Fe_3O_4 [31]	MBR; particles added to sludge and/or membrane surface	Addition location reported; quantitative dose: NR	NR	Particle location assessed qualitatively; compartmental Fe_3O_4 recovery: NR	No	Spatial dosing studied; system-wide Fe_3O_4 balance not established.
TA-Cu/PVDF [21]	Continuous AnMBR	TA:Cu(II) molar ratio = 1:3	NR	Cu confirmed in membrane coating; sludge/cake/biofilm concentrations: NR	No	Performance evaluated; Cu release and reactor-wide partitioning unresolved.
Ag@SiO_2/PVDF [38]	Continuous MBR	107.7 ± 10.9 μg Ag/cm^2	Ag^+ release ≈0.5 μg/(cm^2·d)	Membrane loading quantified; sludge/cake/biofilm Ag concentrations: NR	Partial	Loading/release quantified; reactor-wide Ag balance incomplete.

*Note: NR, not quantitatively reported in the source evidence summarized here. Nominal dose or membrane-surface loading is an input metric, not a phase-distribution measurement. "No" indicates that a reactor-wide balance across liquid, sludge, cake/biofilm, cleaning effluent, and discharge streams was unavailable; "Partial" indicates that at least one quantitative release or fate metric was reported without a closed system balance.

Table 8. Priority-based indicators for the safe application of metal-based functional interfaces.

Assessment level	Priority	Key indicators	Recommended methods	Current evidence boundary
Pollutant	Mandatory	Parent-antibiotic removal; liquid/solid partitioning; TP identity/concentration; residual toxicity	LC–MS/MS/HRMS; mass balance; non-target screening; bioassays	TP quantification, toxicity trajectories, and closed mass balances are uncommon in direct MBR studies
Operational	Mandatory	TMP, flux, permeability, EPS/SMP, cake structure; metal leaching/loss; interface passivation and durability	Fouling-resistance analysis; microscopy; ICP-MS; XPS/XRD; long-term operation	Long-term metal fate, passivation, functional-layer aging, and replacement demand are not well characterized
Engineering-economic	Recommended*	Specific energy consumption; electrode/material consumption and lifetime; OPEX	Energy/material balance; techno-economic and life-cycle cost analysis	Energy demand is condition-dependent, and standardized pilot/full-scale cost data are scarce
Resistance risk	Mandatory	Absolute ARG/MRG abundance; intracellular/extracellular ARGs; MGEs; potential hosts; ARG–MRG linkage	qPCR/dPCR; metagenomics; long-read sequencing; plasmidomics/Hi-C	Host confirmation, ARG–MRG co-localization, and direct HGT measurements remain uncommon
Functional response	Research	Metal-homeostasis/efflux genes; SOS and integrase responses; conjugation frequency	RT-qPCR; transcriptomics/proteomics; conjugation assays	Expression activity and actual dissemination capacity are rarely measured together
Spatial distribution	Recommended	Antibiotic, metal, and ARG/MGE loads in liquid, sludge, cake layers, membrane biofilms, and cleaning effluent	Layer-resolved sampling; microscopy; spatial omics; mass-load analysis	Layer-resolved, system-wide datasets remain scarce
Integrated assessment	Mandatory	Genuine degradation; TP toxicity; membrane stability; metal release; total ARG/MGE dissemination; energy/OPEX	Life-cycle mass balance; multi-indicator normalization; benefit–risk–cost matrix	No cross-platform safety or economic thresholds have been validated for these systems

7. Conclusions and research outlook

7.1. Conclusions and testable hypotheses

The key question for metal-based functional interfaces is no longer whether they can improve antibiotic removal or membrane fouling. The more useful question is when those gains persist without creating a new burden through toxic TPs, metal-driven selection, or internal ARG/MGE accumulation. The literature provides enough evidence to frame that problem, but the datasets remain distributed

across materials, reactor designs, operating times, and analytical endpoints. Four hypotheses offer a direct way to turn those gaps into testable research.

(1) Interfacial aging may control long-term benefit–risk behavior more strongly than initial material properties. EPS coverage, particle aggregation, surface oxidation, and passivation progressively change access to reactive sites and interfacial reactivity [50–52]. What has not been followed directly is how those physical changes map onto antibiotic transformation and resistance response over the same operating period. We hypothesize that an interface can move from synergistic reduction toward risk decoupling or enrichment and transfer as reactive sites become covered, passivated, or redistributed within fouling layers. Testing this state-transition hypothesis requires long-term, layer-resolved measurements of parent antibiotics, TPs, metal speciation, ARGs/MGEs, and interfacial properties in the same reactor.

(2) Local bioavailable exposure may predict resistance selection better than total metal dose or bulk concentration. Fouling layers retain resistance determinants and create chemically and biologically heterogeneous microenvironments [64,68]. Co-selection is also controlled by metal bioavailability, host identity, and physical linkage between ARGs and MRGs, not by total metal abundance [72,73]. We hypothesize that layer-specific bioavailable metal concentrations, residual antibiotics and TPs, and local residence time will explain ARG/MRG enrichment and MGE activity more effectively than bulk-phase measurements. Spatially resolved chemistry should be paired with absolute ARG/MRG quantification, host identification, and direct gene-transfer measurements.

(3) Similar parent-antibiotic removal efficiencies can mask very different environmental outcomes. Direct MBR studies often report strong removal without resolving TP identity, concentration, or toxicity in parallel [23,32,34], while non-MBR mechanistic studies show that transformation can generate multiple intermediates and non-monotonic toxicity profiles [97–99]. We hypothesize that two systems with comparable parent removal may diverge sharply in risk when one is dominated by adsorption and solid-phase transfer and the other by genuine transformation and detoxification. Complete mass balances that include parent compounds, major TPs, residual toxicity, and resistance endpoints are needed to test this directly.

(4) Metal-based strategies are likely to have operating windows, not universally optimal doses or electrical conditions. Performance varies with metal dose, particle-addition mode, and applied electrical conditions [17,23,31]. Functionalized membranes and electrochemical systems add further constraints through long-term metal release, interface deterioration, energy demand, and electrode side reactions [21,38,100]. We hypothesize that each route has a benefit–risk–cost window in which genuine antibiotic transformation and membrane stability are high while metal release, ARG/MGE dissemination, energy use, and material replacement remain acceptable. Mapping that window requires systematic variation of operating conditions in real wastewater over long periods, not isolated optimum points from short tests.

These four hypotheses converge on one experimental need: follow the interface through time and across space while closing the relevant mass balances. The most informative studies will show when a treatment-enhancing interface begins to behave as a pollutant or resistance reservoir, what triggers that transition, and whether operation or cleaning can reverse it. Scale-up then becomes a test of whether the same state transitions remain controllable outside the bench reactor.

7.2. Scale-up from laboratory studies to engineering applications

Most evidence summarized in Table 3 comes from bench-scale MBRs or closely related membrane-coupled reactors; only a small number of technical routes have reached pilot scale. Bench studies establish mechanism and proof of performance more securely than full-scale robustness. At a larger scale, real-wastewater variability, uneven mass transfer and material distribution, module loading, cleaning practice, and sludge management can change the behavior of a metal-based interface. Engineering validation needs to reproduce the full operating cycle, including performance drift, fouling, cleaning, material aging, and downstream residuals. A short-term removal percentage alone cannot support plant-scale extrapolation.

Real wastewater is the first scale-up filter. Competing ligands, variable organic matter, suspended solids, EPS, and biofilm coverage can change antibiotic speciation and metal-interface chemistry [29,50–52]. Fe^{3+} flocculation, nZVI reduction, magnetic-biochar adsorption, or membrane-derived metal release can behave differently from the same process in synthetic feed. Scale-up studies should test stability across water-quality fluctuations, loading changes, and spatial heterogeneity instead of relying on a single controlled influent.

Time is the second filter. Particle aggregation, oxidation, passivation, and EPS coverage can progressively change iron-based interfaces [50–52], while metal-functionalized membranes can alter release behavior and surface function during extended operation [21,38]. A scale-up study should close the metal balance from addition through migration, accumulation, leaching, and discharge, and relate those flows to sludge properties, inorganic deposition, and local selection pressure.

Chemical cleaning is a third filter because it can rebuild the interface while restoring flux. Sodium hypochlorite can alter sludge and EPS properties and accelerate post-cleaning fouling [59]; halotolerant bacteria may survive and contribute to recolonization [60]; and reactions between NaOCl and organic foulants can form disinfection by-products [61]. Long-term tests of metal-functionalized systems should include repeated cleaning cycles and compare metal release, functional-layer integrity, microbial recolonization, and antibiotic/ARG/MGE redistribution before and after cleaning.

The system boundary also extends beyond the membrane tank. Metal-containing sludge, spent cake layers, and cleaning effluents can carry contaminants and resistance determinants into downstream treatment or disposal routes. Sludge processing and resource recovery can further change the fate of metals, antibiotics, ARGs, and MRGs, while land application creates a direct pathway into terrestrial environments [108,109]. Engineering evaluation should include sludge treatment, cleaning-effluent management, and final recovery or disposal streams.

A credible scale-up pathway should build evidence in stages. Bench systems treating real wastewater can define dose and operating windows under representative conditions. Pilot systems can then test start-up, loading shocks, material replenishment, membrane fouling, repeated cleaning, and long-term interface aging. Effluent, sludge, fouling layers, cleaning effluents, and spent materials should enter the same mass balance. Scale-up is credible only when the removal and fouling benefits seen at bench scale remain reproducible under larger hydraulic, mass-transfer, and operational variability while metal fate and resistance risk stay controllable across the full operation–cleaning–disposal cycle.

Author contributions

Zihao Liu: Investigation, data curation, visualization, writing–original draft; Mingchao Zhu: Conceptualization, supervision, project administration, funding acquisition, writing–review and editing; Shuping Li: Investigation, validation, writing–review and editing. All authors have read and approved the final version of the manuscript for publication.

Use of AI tools declaration

The authors declare they have not used Artificial Intelligence (AI) tools in the creation of this article.

Acknowledgments

This work was partially supported by the Science and Technology Projects of Xizang Autonomous Region (No. XZ202501JD0010, XZ202601ZR0173), the Young Scholar Incubation Plan of Xizang Minzu University (No. 25MDX03), and the Scientific Research Program funded by the Education Department of Shaanxi Provincial Government (No. 25JK0704).

Conflict of interest

The authors declare no conflict of interest.

References

1. Baker-Austin C, Wright MS, Stepanauskas R, et al. (2006) Co-selection of antibiotic and metal resistance. *Trends Microbiol* 14: 176–182. https://doi.org/10.1016/j.tim.2006.02.006
2. Seiler C, Berendonk TU (2012) Heavy metal driven co-selection of antibiotic resistance in soil and water bodies impacted by agriculture and aquaculture. *Front Microbiol* 3: 399. https://doi.org/10.3389/fmicb.2012.00399
3. Kümmerer K (2009) Antibiotics in the aquatic environment—A review—Part I. *Chemosphere* 75: 417–434. https://doi.org/10.1016/j.chemosphere.2008.11.086
4. Yu T, Al-Dhabi NA, Xing W, et al. (2025) Highly efficient antibiotic decontamination and biotoxicity elimination with activity-stability considerations via encapsulated catalyst induced peroxymonosulfate activation. *J Environ Manage* 396: 128078. https://doi.org/10.1016/j.jenvman.2025.128078
5. Li X, Xing W, Al-Dhabi NA, et al. (2026) Encapsulated nanoconfined microenvironment and fluorine coordination boost selective peroxymonosulfate activation toward Co(IV)=O dominated high-efficiency pollutant degradation and biotoxicity abatement. *Adv Funct Mater* 36: e75641. https://doi.org/10.1002/adfm.75641
6. Zhu YG, Johnson TA, Su JQ, et al. (2013) Diverse and abundant antibiotic resistance genes in Chinese swine farms. *P Natl Acad Sci USA* 110: 3435–3440. https://doi.org/10.1073/pnas.1222743110

7. Michael I, Rizzo L, McArdell CS, et al. (2013) Urban wastewater treatment plants as hotspots for the release of antibiotics in the environment: A review. *Water Res* 47: 957–995. https://doi.org/10.1016/j.watres.2012.11.027
8. Rizzo L, Manaia CM, Merlin C, et al. (2013) Urban wastewater treatment plants as hotspots for antibiotic resistant bacteria and genes spread into the environment: A review. *Sci Total Environ* 447: 345–360. https://doi.org/10.1016/j.scitotenv.2013.01.032
9. Karkman A, Do TT, Walsh F, et al. (2018) Antibiotic-resistance genes in waste water. *Trends Microbiol* 26: 220–228. https://doi.org/10.1016/j.tim.2017.09.005
10. Ji X, Shen Q, Liu F, et al. (2012) Antibiotic resistance gene abundances associated with antibiotics and heavy metals in animal manures and agricultural soils adjacent to feedlots in Shanghai, China. *J Hazard Mater* 235–236: 178–185. https://doi.org/10.1016/j.jhazmat.2012.07.040
11. Radjenović J, Petrović M, Barceló D (2009) Fate and distribution of pharmaceuticals in wastewater and sewage sludge of the conventional activated sludge (CAS) and advanced membrane bioreactor (MBR) treatment. *Water Res* 43: 831–841. https://doi.org/10.1016/j.watres.2008.11.043
12. Clara M, Strenn B, Kreuzinger N (2004) Carbamazepine as a possible anthropogenic marker in the aquatic environment: Investigations on the behaviour of carbamazepine in wastewater treatment and during groundwater infiltration. *Water Res* 38: 947–954. https://doi.org/10.1016/j.watres.2003.10.058
13. Hai FI, Yamamoto K, Lee CH (2014) *Membrane biological reactors: Theory, modeling, design, management and applications to wastewater reuse*. London: IWA Publishing. https://doi.org/10.2166/9781780401331
14. Judd S (2011) *The MBR book: Principles and applications of membrane bioreactors for water and wastewater treatment*. 2 Eds., Oxford: Butterworth-Heinemann.
15. Meng F, Chae SR, Drews A, et al. (2009) Recent advances in membrane bioreactors (MBRs): Membrane fouling and membrane material. *Water Res* 43: 1489–1512. https://doi.org/10.1016/j.watres.2008.12.044
16. Zhu YJ, Wang YY, Zhou S, et al. (2018) Robust performance of a membrane bioreactor for removing antibiotic resistance genes exposed to antibiotics: Role of membrane foulants. *Water Res* 130: 139–150. https://doi.org/10.1016/j.watres.2017.11.067
17. Zhang L, Bai R, Zhang J, et al. (2025) Fe^{3+} addition as a promising strategy to enhance the pollutant removal performance and mitigate the membrane fouling of a laboratory-scale membrane bioreactor treating sulfamethoxazole wastewater. *Environ Res* 274: 121284. https://doi.org/10.1016/j.envres.2025.121284
18. Madsen JS, Burmølle M, Hansen LH, et al. (2012) The interconnection between biofilm formation and horizontal gene transfer. *FEMS Immunol Med Mic* 65: 183–195. https://doi.org/10.1111/j.1574-695x.2012.00960.x
19. Wang Z, Wu Z, Tang S (2009) Extracellular polymeric substances (EPS) properties and their effects on membrane fouling in a submerged membrane bioreactor. *Water Res* 43: 2504–2512. https://doi.org/10.1016/j.watres.2009.02.026
20. Jarusutthirak C, Amy G (2007) Understanding soluble microbial products (SMP) as a component of effluent organic matter (EfOM). *Water Res* 41: 2787–2793. https://doi.org/10.1016/j.watres.2007.03.005
21. Maneewan P, Sajomsang W, Singto S, et al. (2021) Fouling mitigation in an anaerobic membrane bioreactor via membrane surface modification with tannic acid and copper. *Environ Pollut* 291: 118205. https://doi.org/10.1016/j.envpol.2021.118205

22. Chen LL, Cheng PJ, Ye L, et al. (2020) Biological performance and fouling mitigation in the biochar-amended anaerobic membrane bioreactor (AnMBR) treating pharmaceutical wastewater. *Bioresource Technol* 302: 122805. https://doi.org/10.1016/j.biortech.2020.122805
23. Liu WC, Xia RH, Ding XR, et al. (2022) Impacts of nano-zero-valent iron on antibiotic removal by anaerobic membrane bioreactor for swine wastewater treatment. *J Membrane Sci* 659: 120762. https://doi.org/10.1016/j.memsci.2022.120762
24. Wang KM, Ma H, Shen YX, et al. (2023) Magnetic biochar derived from peanut shells facilitates antibiotic degradation and fouling control in anaerobic membrane bioreactor for antibiotic pharmaceutical wastewater treatment. *J Water Process Eng* 55: 104249. https://doi.org/10.1016/j.jwpe.2023.104249
25. Liu SJ, Wang N, Li Y, et al. (2025) Magnetic biochar-mediated iron reduction synergizes with microbial co-metabolism for enhanced adsorption and in-situ degradation of sulfamethoxazole. *Chem Eng J* 523: 168620. https://doi.org/10.1016/j.cej.2025.168620
26. Zhu X, Yang X, Zang L, et al. (2023) Carbon nano-onions as artificial conductive pili enhanced chloramphenicol degradation in anaerobic membrane bioreactor but increased intI1 abundance. *Water Res* 242: 120263.
27. Huang SJ, Shi XQ, Bi XJ, et al. (2019) Effect of ferric hydroxide on membrane fouling in membrane bioreactor treating pharmaceutical wastewater. *Bioresource Technol* 292: 121852. https://doi.org/10.1016/j.biortech.2019.121852
28. Zhang J, Chua HC, Zhou J, et al. (2006) Factors affecting the membrane performance in submerged membrane bioreactors. *J Membrane Sci* 284: 54–66. https://doi.org/10.1016/j.memsci.2006.06.022
29. Yan L, Yin M, Jiao Y, et al. (2023) The presence of copper ions alters tetracycline removal pathway in aerobic granular sludge: Performance and mechanism. *Bioresource Technol* 385: 129446. https://doi.org/10.1016/j.biortech.2023.129446
30. Sheng GP, Yu HQ, Li XY (2010) Extracellular polymeric substances (EPS) of microbial aggregates in biological wastewater treatment systems: A review. *Biotechnol Adv* 28: 882–894. https://doi.org/10.1016/j.biotechadv.2010.08.001
31. He HY, Xin XD, Qiu W, et al. (2022) Role of nano-Fe_3O_4 particle on improving membrane bioreactor (MBR) performance: Alleviating membrane fouling and microbial mechanism. *Water Res* 209: 117897. https://doi.org/10.1016/j.watres.2021.117897
32. Chen M, Xu J, Dai R, et al. (2019) Development of a moving-bed electrochemical membrane bioreactor to enhance removal of low-concentration antibiotic from wastewater. *Bioresource Technol* 293: 122022. https://doi.org/10.1016/j.biortech.2019.122022
33. Xue Y, Cheng YF, Wang QR, et al. (2024) Simultaneous removal of ammonia nitrogen, sulfamethoxazole, and antibiotic resistance genes in self-corrosion microelectrolysis-enhanced counter-diffusion biofilm system. *Bioresource Technol* 412: 131399. https://doi.org/10.1016/j.biortech.2024.131399
34. Li ZH, Yuan L, Yang CW, et al. (2022) Anaerobic electrochemical membrane bioreactor effectively mitigates antibiotic resistance genes proliferation under high antibiotic selection pressure. *Environ Int* 166: 107381. https://doi.org/10.1016/j.envint.2022.107381
35. Li ZH, Yuan L, Wang L, et al. (2022) Coexistence of silver ion and tetracycline at environmentally relevant concentrations greatly enhanced antibiotic resistance gene development in activated sludge bioreactor. *J Hazard Mater* 423: 127088. https://doi.org/10.1016/j.jhazmat.2021.127088

36. Chen M, Ren L, Qi K, et al. (2020) Enhanced removal of pharmaceuticals and personal care products from real municipal wastewater using an electrochemical membrane bioreactor. *Bioresource Technol* 311: 123579. https://doi.org/10.1016/j.biortech.2020.123579
37. Kinfu HH, Rahman MM (2023) Separation performance of membranes containing ultrathin surface coating of metal-polyphenol network. *Membranes* 13: 481. https://doi.org/10.3390/membranes13050481
38. Zhang XR, Guo Y, Wang TL, et al. (2020) Antibiofouling performance and mechanisms of a modified polyvinylidene fluoride membrane in an MBR for wastewater treatment: Role of silver@silica nanopollens. *Water Res* 176: 115749. https://doi.org/10.1016/j.watres.2020.115749
39. Zhou HM, Dai RB, Wang TL, et al. (2022) Enhancing stability of tannic acid-FeIII nanofiltration membrane for water treatment: Intercoordination by metal–organic framework. *Environ Sci Technol* 56: 17266–17277. https://doi.org/10.1021/acs.est.2c05048
40. Yu SJ, Pang HW, Huang SY, et al. (2021) Recent advances in metal-organic framework membranes for water treatment: A review. *Sci Total Environ* 800: 149662. https://doi.org/10.1016/j.scitotenv.2021.149662
41. Wu H, Xu XY, Shi L, et al. (2019) Manganese oxide integrated catalytic ceramic membrane for degradation of organic pollutants using sulfate radicals. *Water Res* 167: 115110. https://doi.org/10.1016/j.watres.2019.115110
42. Hirani RAK, Wu H, Asif AH, et al. (2023) Cobalt oxide functionalized ceramic membrane for 4-hydroxybenzoic acid degradation via peroxymonosulfate activation. *J Hazard Mater* 448: 130874. https://doi.org/10.1016/j.jhazmat.2023.130874
43. Zang L, Yang XL, Xu H, et al. (2024) A novel integrated microbial fuel cell-membrane bioreactor (MFC-MBR) for controlling the spread of antibiotic and antibiotic resistance genes while simultaneously alleviating membrane fouling. *Chem Eng J* 487: 150578. https://doi.org/10.1016/j.cej.2024.150578
44. Li T, Yang XL, Qin CY, et al. (2024) Role of membrane fouling layer in microbial fuel cell-membrane bioreactor (MFC-MBR) for controlling sulfamethoxazole and corresponding resistance genes. *J Environ Manage* 366: 121876. https://doi.org/10.1016/j.jenvman.2024.121876
45. Zang L, Yang XL, Xu H, et al. (2023) Alleviating membrane fouling by enhanced bioelectricity generation via internal reflux of sludge mixed liquor in microbial fuel cell-membrane bioreactor (MFC-MBR) coupling system. *J Membr Sci* 673: 121495. https://doi.org/10.1016/j.memsci.2023.121495
46. Chen P, Guo XY, Li SN, et al. (2021) A review of the bioelectrochemical system as an emerging versatile technology for reduction of antibiotic resistance genes. *Environ Int* 156: 106689. https://doi.org/10.1016/j.envint.2021.106689
47. Xue W, Li F, Zhou Q (2019) Degradation mechanisms of sulfamethoxazole and its induction of bacterial community changes and antibiotic resistance genes in a microbial fuel cell. *Bioresource Technol* 289: 121632. https://doi.org/10.1016/j.biortech.2019.121632
48. Yan WF, Guo YY, Xiao Y, et al. (2018) The changes of bacterial communities and antibiotic resistance genes in microbial fuel cells during long-term oxytetracycline processing. *Water Res* 142: 105–114. https://doi.org/10.1016/j.watres.2018.05.047
49. Flemming HC, Wingender J (2010) The biofilm matrix. *Nat Rev Microbiol* 8: 623–633. https://doi.org/10.1038/nrmicro2415
50. Stefaniuk M, Oleszczuk P, Ok YS (2016) Review on nano zerovalent iron (nZVI): From synthesis to environmental applications. *Chem Eng J* 287: 618–632. https://doi.org/10.1016/j.cej.2015.11.046

51. Ikuma K, Decho AW, Lau BLT (2015) When nanoparticles meet biofilms—Interactions guiding the environmental fate and accumulation of nanoparticles. *Front Microbiol* 6: 591. https://doi.org/10.3389/fmicb.2015.00591
52. Fulaz S, Vitale S, Quinn L, et al. (2019) Nanoparticle–biofilm interactions: The role of the EPS matrix. *Trends Microbiol* 27: 915–926. https://doi.org/10.1016/j.tim.2019.07.004
53. Whitchurch CB, Tolker-Nielsen T, Ragas PC, et al. (2002) Extracellular DNA required for bacterial biofilm formation. *Science* 295: 1487. https://doi.org/10.1126/science.295.5559.1487
54. Mulcahy H, Charron-Mazenod L, Lewenza S (2008) Extracellular DNA chelates cations and induces antibiotic resistance in Pseudomonas aeruginosa biofilms. *PLoS Pathog* 4: e1000213. https://doi.org/10.1371/journal.ppat.1000213
55. Sheng Z, Liu Y (2011) Effects of silver nanoparticles on wastewater biofilms. *Water Res* 45: 6039–6050. https://doi.org/10.1016/j.watres.2011.08.065
56. Gao WJ, Lin HJ, Leung KT, et al. (2011) Structure of cake layer in a submerged anaerobic membrane bioreactor. *J Membrane Sci* 374: 110–120. https://doi.org/10.1016/j.memsci.2011.03.019
57. Matar GK, Bagchi S, Zhang K, et al. (2017) Membrane biofilm communities in full-scale membrane bioreactors are not randomly assembled and consist of a core microbiome. *Water Res* 123: 124–133. https://doi.org/10.1016/j.watres.2017.06.052
58. Cheng QQ, Lee S, Ren XH, et al. (2024) Spatial variability of cake layer in membrane fouling of full-scale MBR: New insights and implications. *J Environ Chem Eng* 12: 114126. https://doi.org/10.1016/j.jece.2024.114126
59. Sun M, Yan L, Zhang L, et al. (2019) New insights into the rapid formation of initial membrane fouling after in-situ cleaning in a membrane bioreactor. *Process Biochem* 78: 108–113. https://doi.org/10.1016/j.procbio.2019.01.004
60. Navarro RR, Hori T, Inaba T, et al. (2016) High-resolution phylogenetic analysis of residual bacterial species of fouled membranes after NaOCl cleaning. *Water Res* 94: 166–175. https://doi.org/10.1016/j.watres.2016.02.044
61. Wang H, Ma D, Shi W, et al. (2021) Formation of disinfection by-products during sodium hypochlorite cleaning of fouled membranes from membrane bioreactors. *Front Env Sci Eng* 15: 102. https://doi.org/10.1007/s11783-021-1389-3
62. Kappell AD, Kimbell LK, Seib MD, et al. (2018) Removal of antibiotic resistance genes in an anaerobic membrane bioreactor treating primary clarifier effluent at 20 °C. *Environ Sci-Wat Res* 4: 1783–1793. https://doi.org/10.1039/C8EW00270C
63. Zarei-Baygi A, Smith AL (2021) Intracellular versus extracellular antibiotic resistance genes in the environment: Prevalence, horizontal transfer, and mitigation strategies. *Bioresource Technol* 319: 124181. https://doi.org/10.1016/j.biortech.2020.124181
64. Zarei-Baygi A, Wang P, Harb M, et al. (2020) Membrane fouling inversely impacts intracellular and extracellular antibiotic resistance gene abundances in the effluent of an anaerobic membrane bioreactor. *Environ Sci Technol* 54: 12742–12751. https://doi.org/10.1021/acs.est.0c04787
65. Harb M, Zarei-Baygi A, Wang P, et al. (2021) Antibiotic transformation in an anaerobic membrane bioreactor linked to membrane biofilm microbial activity. *Environ Res* 200: 111456. https://doi.org/10.1016/j.envres.2021.111456
66. Wang KM, Zhou LX, Meng SH, et al. (2023) Anaerobic membrane bioreactor for real antibiotic pharmaceutical wastewater treatment: Positive effect of fouling layer on antibiotics and antibiotic resistance genes removals. *J Clean Prod* 409: 137234. https://doi.org/10.1016/j.jclepro.2023.137234

67. Molin S, Tolker-Nielsen T (2003) Gene transfer occurs with enhanced efficiency in biofilms and induces enhanced stabilisation of the biofilm structure. *Curr Opin Biotech* 14: 255–261. https://doi.org/10.1016/s0958-1669(03)00036-3
68. Song YM, Li Y, Li MY, et al. (2026) Fouling layer as a selective reservoir of antibiotic resistance genes: Enrichment and constrained mobility in a methylotrophic anaerobic membrane bioreactor. *J Membrane Sci* 752: 125633. https://doi.org/10.1016/j.memsci.2026.125633
69. Stepanauskas R, Glenn TC, Jagoe CH, et al. (2005) Elevated microbial tolerance to metals and antibiotics in metal-contaminated industrial environments. *Environ Sci Technol* 39: 3671–3678. https://doi.org/10.1021/es048468f
70. Wales AD, Davies RH (2015) Co-selection of resistance to antibiotics, biocides and heavy metals, and its relevance to foodborne pathogens. *Antibiotics* 4: 567–604. https://doi.org/10.3390/antibiotics4040567
71. Berendonk TU, Manaia CM, Merlin C, et al. (2015) Tackling antibiotic resistance: The environmental framework. *Nat Rev Microbiol* 13: 310–317. https://doi.org/10.1038/nrmicro3439
72. Li LG, Xia Y, Zhang T (2017) Co-occurrence of antibiotic and metal resistance genes revealed in complete genome collection. *ISME J* 11: 651–662. https://doi.org/10.1038/ismej.2016.155
73. Pal C, Asiani K, Arya S, et al. (2017) Metal resistance and its association with antibiotic resistance. *Adv Microb Physiol* 70: 261–313. https://doi.org/10.1016/bs.ampbs.2017.02.001
74. Li AD, Li LG, Zhang T (2015) Exploring antibiotic resistance genes and metal resistance genes in plasmid metagenomes from wastewater treatment plants. *Front Microbiol* 6: 1025. https://doi.org/10.3389/fmicb.2015.01025
75. Li B, Qiu Y, Li J, et al. (2019) Removal of antibiotic resistance genes in four full-scale membrane bioreactors. *Sci Total Environ* 653: 112–119. https://doi.org/10.1016/j.scitotenv.2018.10.305
76. Le TH, Ng C, Tran NH, et al. (2018) Removal of antibiotic residues, antibiotic resistant bacteria and antibiotic resistance genes in municipal wastewater by membrane bioreactor systems. *Water Res* 145: 498–508. https://doi.org/10.1016/j.watres.2018.08.060
77. Sun Y, Shen YX, Liang P, et al. (2016) Multiple antibiotic resistance genes distribution in ten large-scale membrane bioreactors for municipal wastewater treatment. *Bioresource Technol* 222: 100–106. https://doi.org/10.1016/j.biortech.2016.09.117
78. Sui Q, Jiang C, Zhang J, et al. (2018) Does the biological treatment or membrane separation reduce the antibiotic resistance genes from swine wastewater through a sequencing-batch membrane bioreactor treatment process. *Environ Int* 118: 274–281. https://doi.org/10.1016/j.envint.2018.06.008
79. Stewart PS (2003) Diffusion in biofilms. *J Bacteriol* 185: 1485–1491. https://doi.org/10.1128/jb.185.5.1485-1491.2003
80. Stewart PS, Franklin MJ (2008) Physiological heterogeneity in biofilms. *Nat Rev Microbiol* 6: 199–210. https://doi.org/10.1038/nrmicro1838
81. Partridge SR, Kwong SM, Firth N, et al. (2018) Mobile genetic elements associated with antimicrobial resistance. *Clin Microbiol Rev* 31: e00088-17. https://doi.org/10.1128/cmr.00088-17
82. von Wintersdorff CJH, Penders J, van Niekerk JM, et al. (2016) Dissemination of antimicrobial resistance in microbial ecosystems through horizontal gene transfer. *Front Microbiol* 7: 173. https://doi.org/10.3389/fmicb.2016.00173
83. Yang D, Wang JF, Qiu ZG, et al. (2013) Horizontal transfer of antibiotic resistance genes in a membrane bioreactor. *J Biotechnol* 167: 441–447. https://doi.org/10.1016/j.jbiotec.2013.08.004
84. Larsson DGJ, Flach CF (2022) Antibiotic resistance in the environment. *Nat Rev Microbiol* 20: 257–269. https://doi.org/10.1038/s41579-021-00649-x

85. Peltier E, Vincent J, Finn C, et al. (2010) Zinc-induced antibiotic resistance in activated sludge bioreactors. *Water Res* 44: 3829–3836. https://doi.org/10.1016/j.watres.2010.04.041
86. Anes J, McCusker MP, Fanning S, et al. (2015) The ins and outs of RND efflux pumps in Escherichia coli. *Front Microbiol* 6: 587. https://doi.org/10.3389/fmicb.2015.00587
87. Nies DH (2003) Efflux-mediated heavy metal resistance in prokaryotes. *FEMS Microbiol Rev* 27: 313–339. https://doi.org/10.1016/s0168-6445(03)00048-2
88. Liu C, Yan H, Sun Y, et al. (2021) Contribution of enrofloxacin and Cu^{2+} to the antibiotic resistance of bacterial community in a river biofilm. *Environ Pollut* 291: 118156. https://doi.org/10.1016/j.envpol.2021.118156
89. Stewart PS, Costerton JW (2001) Antibiotic resistance of bacteria in biofilms. *Lancet* 358: 135–138. https://doi.org/10.1016/s0140-6736(01)05321-1
90. Zheng J, Wang S, Gong Q, et al. (2024) Fate of antibiotic resistance genes and EPS defence mechanisms during simultaneous denitrification and methanogenesis, coupled with the biodegradation of multiple antibiotics under zinc stress. *Water Res* 261: 121996. https://doi.org/10.1016/j.watres.2024.121996
91. Wang P, Zarei-Baygi A, Delgado Vela J, et al. (2023) Metagenomic analysis of the antibiotic resistance risk between an aerobic and anaerobic membrane bioreactor. *ACS EST Water* 3: 1865–1873. https://doi.org/10.1021/acsestwater.2c00383
92. Silver S, Phung LT (2005) A bacterial view of the periodic table: Genes and proteins for toxic inorganic ions. *J Ind Microbiol Biot* 32: 587–605. https://doi.org/10.1007/s10295-005-0019-6
93. Gillings MR, Gaze WH, Pruden A, et al. (2015) Using the class 1 integron-integrase gene as a proxy for anthropogenic pollution. *ISME J* 9: 1269–1279. https://doi.org/10.1038/ismej.2014.226
94. Guerin E, Cambray G, Sanchez-Alberola N, et al. (2009) The SOS response controls integron recombination. *Science* 324: 1034. https://doi.org/10.1126/science.1172914
95. Liu C, Li B, Wu B, et al. (2022) How heavy metal stress promotes dissemination of antibiotic resistance genes in the activated sludge process. *J Hazard Mater* 437: 129279. https://doi.org/10.1016/j.jhazmat.2022.129279
96. Li H, Song HL, Xu H, et al. (2020) Effect of the coexposure of sulfadiazine, ciprofloxacin and zinc on the fate of antibiotic resistance genes, bacterial communities and functions in three-dimensional biofilm-electrode reactors. *Bioresource Technol* 296: 122290. https://doi.org/10.1016/j.biortech.2019.122290
97. Trovó AG, Nogueira RFP, Agüera A, et al. (2009) Degradation of sulfamethoxazole in water by solar Photo-Fenton: Chemical and toxicological evaluation. *Water Res* 43: 3922–3931. https://doi.org/10.1016/j.watres.2009.04.006
98. Dirany A, Efremova Aaron S, Oturan N, et al. (2011) Study of the toxicity of sulfamethoxazole and its degradation products in water by a bioluminescence method during application of the electro-Fenton treatment. *Anal Bioanal Chem* 400: 353–360. https://doi.org/10.1007/s00216-010-4441-x
99. Zhu K, Qin WL, Gan YP, et al. (2023) Acceleration of Fe^{3+}/Fe^{2+} cycle in garland-like MIL-101(Fe)/MoS_2 nanosheets to promote peroxymonosulfate activation for sulfamethoxazole degradation. *Chem Eng J* 470: 144190. https://doi.org/10.1016/j.cej.2023.144190
100. Asif MB, Maqbool T, Zhang Z (2020) Electrochemical membrane bioreactors: State-of-the-art and future prospects. *Sci Total Environ* 741: 140233. https://doi.org/10.1016/j.scitotenv.2020.140233

101. Shanableh A, Bhattacharjee S, Alani S, et al. (2021) Assessment of sulfamethoxazole removal by nanoscale zerovalent iron. *Sci Total Environ* 761: 143307. https://doi.org/10.1016/j.scitotenv.2020.143307
102. Krawczyk K, Silvestri D, Nguyen NHA, et al. (2022) Enhanced degradation of sulfamethoxazole by a modified nano zero-valent iron with a β-cyclodextrin polymer: Mechanism and toxicity evaluation. *Sci Total Environ* 817: 152888. https://doi.org/10.1016/j.scitotenv.2021.152888
103. Lee D, Kim S, Tang K, et al. (2021) Oxidative degradation of tetracycline by magnetite and persulfate: Performance, water matrix effect, and reaction mechanism. *Nanomaterials* 11: 2292. https://doi.org/10.3390/nano11092292
104. Hou L, Wang L, Royer S, et al. (2016) Ultrasound-assisted heterogeneous Fenton-like degradation of tetracycline over a magnetite catalyst. *J Hazard Mater* 302: 458–467. https://doi.org/10.1016/j.jhazmat.2015.09.033
105. Hai H, Xing X, Li S, et al. (2020) Electrochemical oxidation of sulfamethoxazole in BDD anode system: Degradation kinetics, mechanisms and toxicity evaluation. *Sci Total Environ* 738: 139909. https://doi.org/10.1016/j.scitotenv.2020.139909
106. Dickinson AW, Power A, Hansen MG, et al. (2019) Heavy metal pollution and co-selection for antibiotic resistance: A microbial palaeontology approach. *Environ Int* 132: 105117. https://doi.org/10.1016/j.envint.2019.105117
107. Manaia CM, Rocha J, Scaccia N, et al. (2018) Antibiotic resistance in wastewater treatment plants: Tackling the black box. *Environ Int* 115: 312–324. https://doi.org/10.1016/j.envint.2018.03.044
108. Buta M, Hubeny J, Zieliński W, et al. (2021) Sewage sludge in agriculture—The effects of selected chemical pollutants and emerging genetic resistance determinants on the quality of soil and crops—A review. *Ecotox Environ Safe* 214: 112070. https://doi.org/10.1016/j.ecoenv.2021.112070
109. Xie WY, McGrath SP, Su JQ, et al. (2016) Long-term impact of field applications of sewage sludge on soil antibiotic resistome. *Environ Sci Technol* 50: 12602–12611. https://doi.org/10.1021/acs.est.6b02138



AIMS Press

© 2026 the Author(s), licensee AIMS Press. This is an open access article distributed under the terms of the Creative Commons Attribution License (https://creativecommons.org/licenses/by/4.0)